Modeling Fused Filament Fabrication Machine Height Accuracy Through Layer Thickness Variation

Pantelis Gkaliamoutsas

B.S. in Mechanical Engineering with a Concentration in Innovation
B.A. in Economics
Boston University, 2015

Submitted to the Department of Mechanical Engineering in partial fulfillment of the requirements for the degree of

Master of Engineering in Advanced Manufacturing and Design
at the
MASSACHUSETTS INSTITUTE OF TECHNOLOGY

September 2017

Signature redacted

Signature of Author: _____

Department of Mechanical Engineering
August 11, 2017

Signature redacted

Certified by: _____

David E. Hardt
Ralph E. and Eloise F. Cross Professor of Mechanical Engineering
Thesis Supervisor

Signature redacted

Accepted by: _____

Rohan Abeyaratne
Quentin Berg Professor of Mechanics
Chairman, Committee on Graduate Students

This page is intentionally left blank.

Modeling Fused Filament Fabrication Machine Height Accuracy Through Layer Thickness Variation

by

Pantelis Gkaliamoutsas

Submitted to the Department of Mechanical Engineering on August 11, 2017 in Partial Fulfillment of the Requirements for the Degree of Master of Engineering in Advanced Manufacturing and Design

ABSTRACT

This thesis addresses the modeling and prediction of total height error of a 3D printed part using a layer-by-layer approach. Layer to layer thickness error is modeled across the build height of Polyactic acid (PLA) and Acrylonitrile butadiene styrene (ABS) parts. A height error compensation model is then formulated and applied at a G-code level to drive the machine to print accurate parts.

Preliminary experimentation was done on New Valance Robotics' two fused deposition modeling machine versions, the NVPro and the NVPro High-temp. Results suggested that the layer thickness approach was a viable technique for predicting total part height error. The compensation model for PLA parts was also tested and the compensated parts were significantly closer to the expected part height than the uncompensated prints. However, further experimentation will need to be carried out to solidify a model for ABS parts.

Recommendations for future work, measurement method improvement, and model applications are also discussed.

Thesis Supervisor: David E. Hardt
Title: Ralph E. and Eloise F. Cross Professor of Mechanical Engineering

This page is intentionally left blank.

Acknowledgments

I would firstly like to thank my adviser, Professor Hardt, for his guidance, patience, encouragement, and sense of humor that made this thesis experience enjoyable and fulfilling.

I would like to thank the team at NVBOTS, and especially Arjun Chandar, for their passion, and optimism over the past few months. Their friendliness, flexibility and willingness to help made this thesis truly memorable.

I would like to thank my teammates Shien-Yang Lee and Yuanhan Xu for being a pleasure to work with and teaching me invaluable skills along the way.

I would like to thank my parents, Stergios and Eleftheria, and my brother Stefanos for their unwavering love and support. Without them I would not be who I am today.

And finally I would like to thank my girlfriend Frances for her unequivocal love and encouragement that keep me striving to do better.

This page is intentionally left blank.

Contents

This page is intentionally left blank.

List of Figures

This page is intentionally left blank.

List of Tables

This page is intentionally left blank.

List of Abbreviations

ABS+ - Acrylonitrile Butadiene Styrene
ANOVA - Analysis of variance
ANOVACOVA - Analysis of covariance

CAD - Computer aided design
CI - Confidence intervals
CMM - Coordinated measuring machine
CSV - Comma separated values (excel file type)

DOE - Design of experiments

FFF - Fused filament fabrication

FDM - Fused deposition modeling

HT - High-temperature

LTE - Layer thickness error

MEng - Master of Engineering
MIT - Massachusetts Institute of Technology

NVBOTS - New Valance Robotics Corporation

PAE - Printer accuracy experiment
PI - Prediction intervals
PLA- Polyactic Acid

STL - STereoLithography file format (3D Systems)

QC - Quality control

Chapter 1

Introduction

1.1 Purpose

The goal of this thesis is to model the effects of various 3D printer and printed part parameters on the layer thickness variation for different qualified printer materials. This is crucial due to the impending need for greater printer dimensional accuracy. An improvement in dimensional accuracy and consistency will elevate the quality of 3D printing as a manufacturing process. The layer thickness variation ultimately affects the printed total part height accuracy. The possible parameters to be tested are build height, infill density, infill structure, print quality (nominal layer thickness, extrusion speed, nozzle speed), and print material.

1.2 MIT and New Valance Robotics (NVBOTS) Collaboration

This thesis presents one of the three projects undertaken by the MIT Masters of Engineering (MEng) team. The team consisted of three students that each tackled a different problem concerning 3D printing. Yaunhan Xu [1] ex-

plored methods to improve the estimation for time taken to complete a print. Pantelis Gkaliamoutsas and Shien-Yang Lee [2] investigated approaches in increasing the z-dimensional accuracy of 3D printed parts.

1.3 Fused Filament Fabrication

Fused Filament Fabrication, also known as Fused Deposition Modeling (FDM), is a 3D additive manufacturing process whereby a thermoplastic is extruded through a nozzle as a semi-molten filament and is deposited on to a print bed [3]. The extrusion head of the FDM machine typically moves in the x (left-right) and y (front-back) axes depositing layers of material. Once the horizontal layer is extruded, the bed shifts in the z (vertical) axis thus allowing for the next layer to be deposited on top of the preceding layer. Depending on the geometry of the printed part, support material and infill material will need to be added to keep the print from failing. The added material also keeps the part from warping and provides the finished product with extra tensile strength. Once the part has been printed, it is often manually removed and the support material is removed by hand or dissolved in a water-based solution. Depending on the required finish or specified feature geometries of the part it might require post machining before it can be put to its intended use.

1.4 FDM Printing in the Professional Market

A variety of FDM printers are commercially available. The printers range in build envelope size, price, resolution, associated software, qualified print materials, surface finish quality, customization ability, and dimensional accuracy. Desktop consumer 3D printers are often small and have price ranges in the low thousands of dollars. The material choice is limited and the dimensional accuracy is not highly regarded [4]. Professional printers are often

priced at well above $50,000, have build envelopes in excess of 1,500 in^3, and can usually print in a variety of qualified materials. Yet one of the most pressing needs in the professional market is a printer that can repeatedly reproduce high quality and dimensionally accurate parts that can be used in real world engineering applications. A study conducted by Stratasys claims that high-end FDM printers often have dimensional accuracies of $\pm 0.089mm$ or $\pm .0015mm/mm$, whichever is higher[5].

1.5 New Valance Robotics

New Valance Robotics (NVBOTS) is a 3D printing company founded out of the Massachusetts Institute of Technology in 2014, located in South Boston, MA. They manufacture Fused Filament Fabrication (FFF) printers targeted at fulfilling needs in both the educational and commercial markets. Through their automated FFF machines and their cloud based software connecting all their printers, NVBOTS is attempting to build a globally distributed network of smart and automated additive manufacturing machines [6]. The NVCloud offers users the ability to remotely upload print jobs to any printer in their accessible network, adjust its print setting and parameters (such as infill density and print quality), and approve the part for printing. While the printer is active, users can monitor parts' print progress online and be notified if a failure occurs. Additionally, the NVCloud interface makes spool replacement, BuildTak[1] replacement, and self servicing of the printer easy and straightforward.

[1]Thin film material used to separate part from build platform

1.6 The NVPro Printer

1.6.1 Machine Overview

The NVPro printer is a single extrusion FDM machine with maximum print dimensions of $20cm \times 19cm \times 24cm$ [7]. It is differentiated from other plastic FDM machines in the market because of its patented automated part removal system[6]. It has been certified to print in both Polyactic Acid (PLA) and Acrylonitrile Butadiene Styrene (ABS). Currently, NVBOTS engineers and partnering material developers are attempting to certify many more thermoplastics and carbon based polymers such as Ultem (Polyetherimide) and nylon.

The NVPro has a heated print bed, actuated in the z-direction by a lead screw connected through a belt to a stepper motor. The print bed is placed on kinematic coupling for repeatability. For most PLA filament, the nozzle is heated to approximately 220°C while the bed is kept at 50°C. The nozzle extrudes liquid filament onto the bed layer by layer. The hot-end, which contains the nozzle, actuates in the x and y directions using steppers and belt drives. Once the layer has been fully deposited, the hot-end moves off the build platform, a picture is taken by the camera mounted on the frame, and the motor actuates the bed down by a height equal to the nominal layer thickness. Once the part is finished, the bed is lowered to the bottom where the automated removal blade cuts across the top of the bed to scrape the completed part off. It then pushes the part into the finished parts bin before the print bed is zeroed and the next print in the queue is started.

1.6.2 NVCloud and the User Interface

A significant portion of NVBOTS' business comes from their software development. Their cloud-based print control system, NVCloud, allows them to monitor the status of every printer in-house and out in the field. It provides

NVBOTS with real-time data on nozzle and bed temperatures, extrusion parameters, and remaining filament. It also allows NVBOTS to diagnose and track failure modes on each printer.

The NVCloud provides the customer an easy-to-use interface (UI) pictured in Figure 1.1. Through the UI, the user can upload their own customized parts (or parts from NVBOTS' large part library) onto any printer, choose the print settings for that part, and approve it for printing. They can then monitor its progress using the live feed and real-time temperature readings of the print bed and nozzle. On top of this, the UI can be used for self-servicing the printer. The client can run maintenance procedures on the machine such as "Unjamming"[2] the nozzle and replacing the filament.

1.7 Printer and Part Parameters

A variety of print parameters are made available through the NVCloud, as shown in Figure 1.1. The altering and configuration of these parameters can ultimately play major roles in the visual quality, strength, dimensional accuracy, and even the printability of the part. By altering the print parameter options, users can optimize material cost and print time to adhere to their specific requirements.

1.7.1 Material Infill

The NVPro printer allows the user to choose a variety of print options for their 3D part. The infill density of the printed part can be selected over a range of 0% to 75% solidity. This determines how much internal support material will be deposited within the shell of the part. The higher the density, the more solid and heavy the part is, and typically the stronger it is. The infill structure can also be adjusted to take four different types of geometries

[2]NVBOTS' terminology describing the process by which the nozzle is unclogged

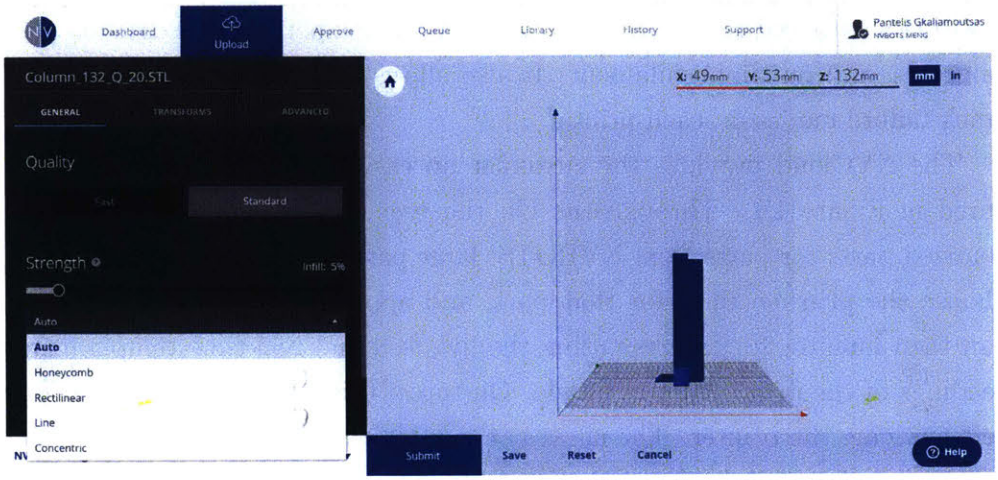

Figure 1.1: NVCloud UI with print options

including honeycomb, rectilinear, linear, and concentric. The different infill structures will affect the sinking of the layers differently and the strength of support between the walls of the shell. NVBOTS' default infill structure is set to honeycomb and it is the infill structure that is deemed most reliable.

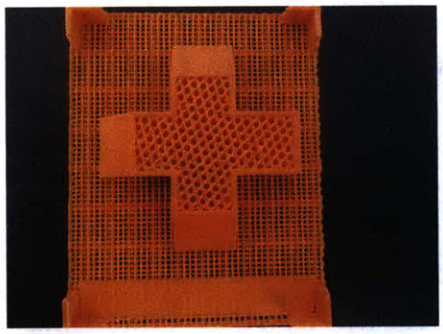

Figure 1.2: Cross-sectional view of column with a 35%, Honeycomb infill structure

1.7.2 Build Height

The build height, across which the layer thickness measurements are taken, is important in determining a relationship over the NVPro's full z-axis operating range. Build height refers to the total height of the printed part. A robust relationship between build height and layer thickness variation can aid in the creation of an accurate compensation model.

1.7.3 Print Quality

The NVCloud allows for three different print quality options: low, standard, and high. The quality chosen determines a variety of printer settings and their configuration such as layer thickness and extrusion speed. For PLA, standard prints have a nominal layer thickness of $0.2mm$ after a first extruded layer of $0.3mm$. Fast quality extrudes nominal layers of $0.3mm$ thicknesses. These are the layer thickness settings that NVBOTS has deemed appropriate and reliable for the various qualities of print. The layer thickness setting is crucial as it effects the adhesion of the part as well the resolution of the printer.

1.7.4 Print Material

With the introduction of a new NVPro high-temperature (HT) printer, the material print capabilities have greatly expanded. NVBOTS has been able to successfully print parts in PLA, ABS+, NylonX, and some carbon infused polymers. Various calibration settings were tested for these materials by the materials engineers at NVBOTS to optimize print time and quality. Based on the reliability of these materials, PLA and ABS+[3] were used as the main focus of this study. ABS+ was printed with the optimal calibration settings that most closely resemble those used for a PLA standard quality print. The

[3]Name of ABS material variation used at NVBOTS

ABS+ nominal layer thickness was set at $0.21167mm$. Due to the timing of the release of the NVPro HT, and the cost and time taken to print ABS+, fewer ABS+ parts were printed for the experiment.

1.7.5 Parameter Ranges and Options

Table 1.1 shows the options available for printing based on the build envelope of the printer and the NVPro dashboard options selection.

Table 1.1: Print parameter options available

Parameter Options	
Build height	0 - 240 mm
Infill density	5% - 75%
Infill structure	Honeycomb / Rectilinear / Line / Concentric
Print quality	Standard / Fast(PLA only)

1.8 Certified Print Materials

NVBOTS has set a vision for their company whereby they will allow users to print "any part, in any material, any time, anywhere"[6]. Having greatly succeeded in establishing three of those four promises through the NVCloud software, the NVBOTS' engineering team has switched focus. They are currently working towards certifying the NVPro HT for use with a variety of different print materials mentioned in Section 1.7.4. The main focus is to calibrate the settings of a HT printer for ABS+ and other new materials. The settings are primarily adjusted to print a visually high quality part that retains easy peal-ability using the automated removal system. Yet dimensional accuracy of these new material parts has not been verified.

1.9 From Design to Print

The design of a part is performed using Computer Aided Software (CAD). The CAD file is then converted into a STereoLithography (STL) part file. In order to 3D print an STL part file, the file must be sliced. NVBOTS calibrates the slicer settings of every batch of filament it uses and sells. This is done to ensure optimal print quality and layer adhesion. Based on the printer and part parameters, the material used, and the slicer settings, a slicer configuration is established. Using this configuration, the STL file is converted into a sliced part file before being translated into G-code. G-code is a numerical control programming languages that sends commands to the printer in order to print a part [9]. Commands include actuating speed, feed rate of material, x and y nozzle position, and print bed z position. The printer interprets these commands and builds the part. Errors can arise between the G-code commands sent to the printer and the actual actions of the printer, causing dimensional inaccuracies in part height.

This page is intentionally left blank.

Chapter 2

Research Motivation

2.1 Competing in the Professional Market

To compete in the professional market, a 3D printing company must produce a printer that must achieve dimensional accuracy abilities similar to those of high-end production 3D printers. Ideally, this is achieved without greatly increasing the price of the printer and by avoiding major hardware changes.

2.2 Interviews and Internal Research

Interviews were conducted with all NVBOTS employees in the hardware engineering, software engineering, customer technical support, marketing, and business divisions of the company. The interviews not only served as a means to learn about the company's policies, products, services, and strategies, but also as a primary diagnosis of general engineering issues faced by the company concerning the NVPro printer. The interviews allowed the MEng team to devise a group of problems that could be worked on as part of the thesis effort. The team then shuffled through data and documents provided by the NVBOTS team.

The primary focus was on dissecting the failure occurrence data which is

tracked and stored by the NVCloud. From this data, it was evident that one of the primary issues was serviceability of the printer. It seemed that clients were struggling to replace hot ends, or unjam nozzles by themselves. Though this was a pressing concern, it would have required redesigns and hardware changes to the NVPro. At the time of writing this thesis, the NVBOTS management was not willing to undertake such an investment. Instead the focus turned to two other needs that, if resolved, would elevate the quality of the NVPro to new heights and allow it to compete with some of the best commercial FDM printers in the market.

The two problems chosen to be tackled by the MEng team were, improving the print time estimation outputted by the current simulator being tested out by NVBOTS, and improving the z-dimensional accuracy of printed parts on the NVPro. The former is explored in Yuanhan Xu's thesis "Modeling Print Time for a Fused Deposition Modeling Machine" [1]. The latter is detailed below.

2.2.1 Z-dimensional Accuracy and Layer Thickness

The z-dimensional accuracy of an FDM printer is based on the consistency in extruded layer thickness as layers are stacked on top of each other. Because layers are of fixed thickness values, the actual part height is not necessarily quantized to plus or minus that value. For example, if the layer thickness in the slicer settings is set to $0.3mm$ and a $5mm$ part is being made, the slicer will over compensate by adding an additional layer which will push the part height to $5.1mm$, thus making the part height divisible by the nominal layer height of $0.3mm$. Yet even parts that are designed to account for such deviations are quite often inaccurate in the z-dimension as is shown in Figure 2.1. Modeling the reason for this inaccuracy will allow for adoption of corrective systems for variations in the layer thickness. This should ultimately lead to repeatable production of highly accurate parts. Caution will be used to try and maintain similar or improved print precision as accuracy is increased.

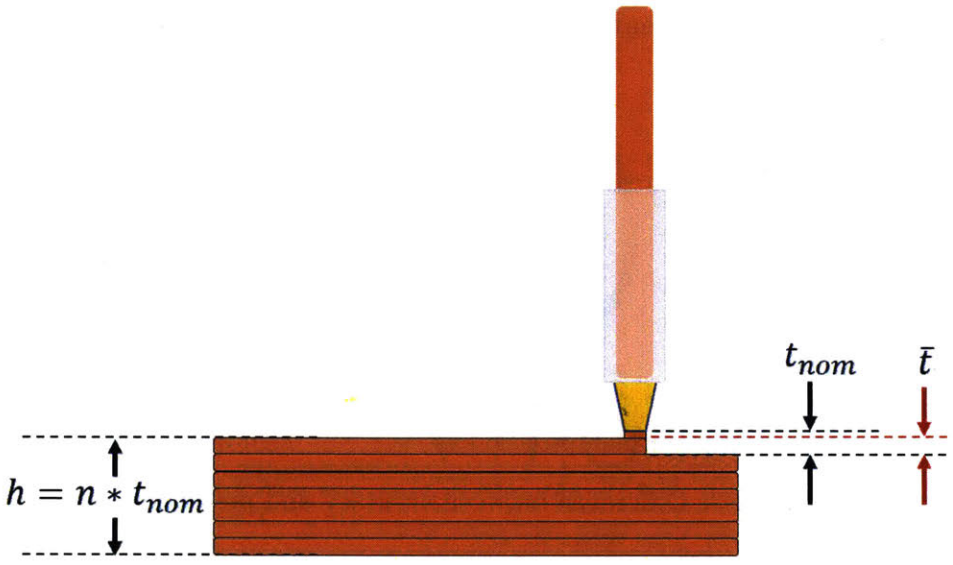

Figure 2.1: Schematic showing the nominal layer thickness, t_{nom}, vs. the actual average layer thickness, $\bar{t}$, and the height of the part, h, based on the layer thickness quantization in FDM printing. n defines the number of layers in the part

2.2.2 Accuracy and Precision

As stated above, the goal of these two theses are to model the accuracy error of the printer and provide compensation methods and models to improve the z-dimensional accuracy of the NVPro. Accuracy refers to how close the measured value is to the nominal or true expected value [10]. In this case this refers to the error in height between the actual measured part and the nominal height set by the slicer. Precision refers to how close the measured values are to each other, i.e. the variation between to similar parts. In order to increase precision of the NVPro, printing noise will have to be reduced to get consistent part geometries. Increasing accuracy on the other hand requires a shift in the mean measured values of the part heights in order to approach a height error of zero. The schematic below explains the difference

between precision and accuracy.

(a) High accuracy with low precision

(b) Low accuracy with high precision

(c) High accuracy with high precision

Figure 2.2: Difference between accuracy and precision

2.2.3 Solutions Considered

Two approaches were considered and pursued. The first was tackled by Shien-Yang Lee in his thesis "Height Error Mapping and Compensation for a Fused Filament Fabrication Machine" [2]. Lee seeks to map height error in all three dimensions across the build envelope. By mapping the error, a compensation model can be formulated and tested using a software based compensation method to try and increase the part height accuracy of the NVPro [2]. The second accuracy approach tackles height dimensional accuracy by modeling variations in layer thickness along the height of a part. This approach is explored in this document.

2.3 Problem Statement and Implications of Research

The second approach involves testing the layer to layer thickness error, across the entire z-dimension, against a variety of print materials, build heights, in-

fill structures, infill densities, and print qualities. By modeling the layer thickness error (LTE) across these parameters, a compensation model can be derived to increase the accuracy of parts printed with varying settings. The z-dimensional accuracy can then be improved through feed-forward compensation of layer thickness variation. This would allow for a software based compensation that would enable NVBOTS to retain the same hardware it currently uses and stocks for the NVPro.

This page is intentionally left blank.

Chapter 3

Prior Work and Literature Review

3.1 NVBOTS Printer Accuracy Experiment (PAE)

The NVBOTS engineering team performed a large dimensional printer accuracy experiment to examine the accuracy of the printer when printing PLA parts [11]. The test encompassed accuracy results in all three axis directions from parts built on six different printers with five or more replicate parts. Figure 3.1a shows the height measured using a coordinated measuring machine (CMM)[1]. The nominal height was subtracted form this measured height to arrive at the part accuracy error. From the initial results, the team came to two important conclusions. Firstly, the printer to printer variation in accuracy was insignificant according to the data collected in all directions. Secondly, the dimensional variation in the z direction was orders of magnitude greater than the dimensional accuracy in the x and y directions. After discussions between the NVBOTS and MEng teams, it was concluded that

[1]Model: TESA Micro-Hite 3D CMM

a simple linear regression was to be fitted to the data of z-axis height error versus total part height. Figure 3.1b shows the scatter of the complete data set with the best fit line.

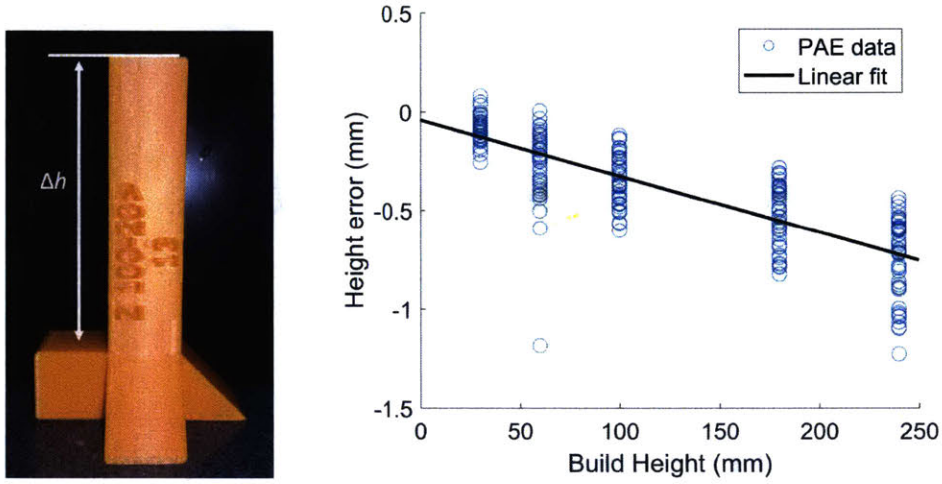

(a) Column design and measurement target

(b) Height error for all parts and linear regression

Figure 3.1: NVBOTS' printer accuracy experiment

3.2 FDM Layer Thickness Variation Analysis

Based on the results given by the NVBOTS dimensional accuracy study, the preliminary work performed by the MIT MEng 2017 NVBOTS team was on printer z-height accuracy. The goal was to model the height error by examining the effect of build height and infill density on layer thickness variation. A step pyramid was designed to allow for a multilevel, 2-factor experimentation shown in Figure 3.2a. Using regression and analysis of variance (ANOVA) [12], it was determined that infill density is statistically insignificant in determining thickness variation. Build height, on the other hand, is linearly

significant within a 96% confidence interval [13]. This simplified the model to just include build height. A quadratic relationship between build height and layer thickness (shown in Figure 3.2b) was established. This relationship only covers a small z-dimensional operating range ($53mm$ of $240mm$) [7] of the NVPro printer.

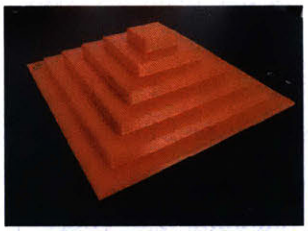

(a) Test part design

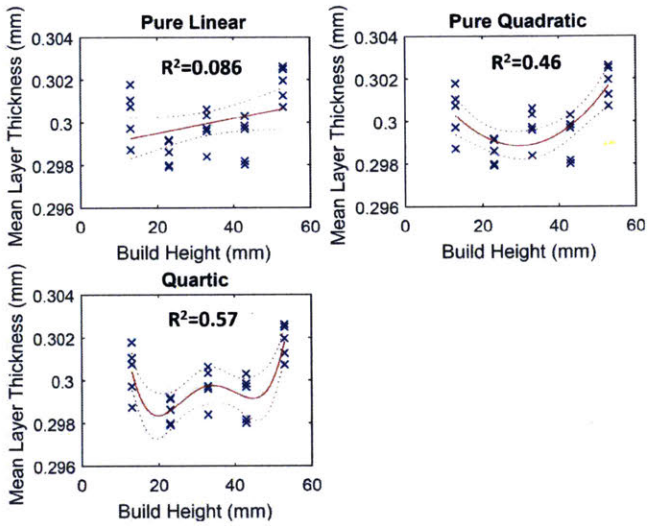

(b) Fitted models between layer thickness and build height

Figure 3.2: MEng team preliminary layer thickness variation experiment [13]

3.3 Causes of Height Inaccuracies

3.3.1 Viscoelastic and Elastic Effects

PLA layer distortions in FDM printing are the main causes of layer thickness variation according to Xinhua et al [14]. Thermal stresses and strains of the PLA form as it is extruded at a hot temperature and is rapidly cooled to ambient temperature [14]. The variation can be explained by the variability

in cooling time between layers at different heights of the part [15]. Zhang et al. [16] also point out that at higher nominal layer thicknesses, the overall cooling rate is lower and less controlled. Less control of cooling rates in the FDM process can cause unpredictable viscoelastic effects in the part causing it to be inaccurate. Elastic effects, due to gravitational pressures from stacked material, are also present. However, according to Costa et al. [17], these effects are negligible in comparison to the effects caused by viscoelastic behavior.

3.3.2 Part and Printer Characteristics

In the paper by Sood et al. [18], the Grey Taguchi Method is used to improve dimensional accuracy of the FDM process. The effect of five printer setting factors on three dimensional accuracy is examined. The factors include layer thickness, part build orientation, raster angle, air gap, and raster width. It is concluded that to fully correct for FDM inaccuracies, optimal factor level settings must be found that do not solely take into consideration significant effects. The use of the Grey Taguchi method allows combining the goals of reducing inaccuracies of all dimensions into a single objective known as the grey relation grade. Maximizing this relation provides optimal factor level settings for dimensional accuracy. The paper also concludes that a lower layer thickness ultimately reduces the percentage change in height of the part whilst also increasing errors in the x and y dimensions.

This notion is backed by Pfeifer et al. [19]. Their attempt to model part quality based on various printer settings resulted in the conclusion that actual printed layer thickness is typically below the expected layer thickness stated in the print settings. They found the biggest variation existed above a layer thickness of $0.35mm$. Though the error is lower at layer thicknesses of $.15mm$ - $3.5mm$, it is still significant and will accumulate to a large inaccuracy across the build height of the part. Concurrently, path width deviation, described as the error in expected width of a single extrusion line, also grew with

higher layer thickness settings [19]. In addition, Akande [20] concludes in his study that layer thickness is the most significant factor to part dimensional accuracy, whilst the interaction between factors infill density and extrusion speed are significant for surface roughness.

3.4 Error Compensation Strategies

3.4.1 Cycle-to-Cycle Feedback Control

Given inaccuracies with part dimensions, two methods of compensation were researched. Cycle-to-Cycle (CtC) feedback is the process by which changes are made to the process after measuring the part, once a cycle is complete [21]. This methodology can be implemented at a layer-by-layer level when it comes to FDM. Once the printer completes the deposition of one layer (one cycle), the current part height can be measured, and compensation can be applied to the next layer. This method repeats until the part is complete. The method has been proven to work and center the process around the expected mean [22].

The largest obstacle in implementation of CtC is that major hardware changes would need to be made to accurately use this strategy. Other issues include measurement and controller delays [21] that would decrease the speed of the FDM process. Finally, CtC will cause higher variance as the loop gain increases. The process will center around the mean value but parts will be more varied.

3.4.2 Feedforward Control

The second method of compensation is one that is explored by Lee[2] [2] and is utilized in this thesis. Feedforward control works by compensating a part before it is printed. This assumes that some prior knowledge of the part

[2]Compensation method is explained in Section 5.1

and process exists that can make an intelligent prediction of error [23]. This control strategy is often model based. In this thesis, the LTE will be modeled and used, through a feedforward control algorithm, to center the process around a mean total part height error of $0mm$.

Chapter 4

Polyactic Acid (PLA) Experiment

4.1 Goal of Experiment

The goal of the PLA experiment is to model the overall part height deviation by taking layer-to-layer thickness deviation across the part's build height. In addition to part build height, print settings such as infill density were tested as a predictive variable with infill structure and print quality serving as categories being modeled. Infill density was factored in again over this wider operating range, despite results from previous experiments pointing to its insignificance.

4.2 Experimental Method

The following experiments were designed to determine the parameters and printer settings significant to the LTE of PLA parts. These were conceived while taking into account past project results discussed in Chapter 3.

4.2.1 Curvature Test

The initial findings from the FDM layer thickness variation analysis experiment show that infill density is not significant, where as build height is highly significant with a possible linear or quadratic relationship to layer thickness variation. Given this result, a small 7-part experiment was designed using columns to test whether curvature exists in relating layer thickness and build height. This experiment featured a two level, single factor Design of Experiments (DOE) with 5 center points (2^1 with 5 CP). This tested the 2 extreme values (levels) of the build height (factor) whilst also examining 5 replicated parts representing a value between the extremes (center points) [24]. The extreme levels of build height tested were $24mm$ and $240mm$

4.2.2 Quality and Infill Density

The second experiment was designed to determine the significance of print quality and its interaction with infill density on layer thickness variation. Although infill density was determined as statistically insignificant for the fast quality during the FDM Layer Thickness Variation Analysis experimentation, it was uncertain whether this would hold true for standard quality parts. It was thus included as an effect. Build height was kept as an effect due to its high significance from past experimentation.

The DOE is shown in Table 4.1. This was a full factorial experiment with 4 center-points for each print quality.

4.2.3 Infill Density and Structure

The third round of experimentation involved testing main effects and interaction effects between infill density, infill geometric structure, and build height. Since all previous columns had been printed with a honeycomb infill structure (NVPro default), the new parts only featured the three other

Table 4.1: 2^3 DOE experiment for print quality with 4 replicates at each center point

	Build height		**Infill density**		**Print quality**	
	high/low	*mm*	high/low	%	high/low	Fast/Standard
(1)	-	24.0	-	5	-	Fast
a	+	240	-	5	-	Fast
b	-	24.0	+	35	-	Fast
ab	+	240	+	35	-	Fast
c	-	24.0	-	5	+	Standard
ac	+	240	-	5	+	Standard
bc	-	24.0	+	35	+	Standard
abc	+	240	+	35	+	Standard
center-point * 4	+	132	+	20	+	Fast
center-point * 4	+	132	+	20	+	Standard

structure options which are Rectilinear, Concentric, and Linear. The DOE of new parts is shown in Table 4.2.

Table 4.2: $2^2 * 3$ DOE experiment for infill structure

Build height		**Infill density**		**Infill Structure**
high/low	*mm*	high/low	%	R/C/L
-	24.0	-	5	Rectilinear
-	24.0	-	5	Concentric
-	24.0	-	5	Linear
+	240	-	5	Rectilinear
+	240	-	5	Concentric
+	240	-	5	Linear
-	24.0	+	35	Rectilinear
-	24.0	+	35	Concentric
-	24.0	+	35	Linear
+	240	+	35	Rectilinear
+	240	+	35	Concentric
+	240	+	35	Linear

4.2.4 Test Part Design

The columns were designed to cover the full operating range of the printer in the z-axis, as well as totaling up to heights that were divisible by the given nominal layer thickness from the slicer. The columns were designed with a cross shaped base for part support and to maximize the stability of the tall columns as they were being printed. The distance between the reference plane and the target plane was kept constant at $9.9mm$ over all column sizes for the curvature experiment (to match the FDM Layer Thickness Variation Analysis experiment). It was then adjusted to $6mm$ for all other parts to provide a more accurate sample error of layers. The rendered CAD model of the part is shown in Figure 4.1.

The short-end of the envelope was tested using $24mm$ target parts and the tall-end is tested using a $240mm$ column. A label was added to each part to distinguish them when collecting them from the completed part bin.

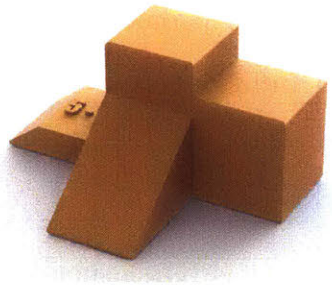

Figure 4.1: Rendered CAD model of $24.0mm$, 5%, fast quality column

4.2.5 Measurement method

NVBOTS owns and operates a TESA Micro-Hite 3D Coordinated Measuring Machine(CMM), shown in Figure 4.2a used for part dimensional quality testing. This precision measurement tool was used to accurately measure part

height and perpendicular distances between target and reference planes in order to provide average estimates of layer thickness between the two planes. To gather such a measurement result, the $5mm$ CMM probe was automatically calibrated using a calibration sphere. The parts were then mounted one at a time on the CMM bed as shown in Figure 4.2b. The probe was lowered by hand onto the reference plane of the part on which 8-10 point measurements were taken. These were stored and a plane was fitted to the data by the CMM while reporting the flatness and z-position of the planar centroid. Similarly, the top plane of the column was measured. This process, from calibration to measurement of the top plane, was repeated three times for each part to test the measurement method repeatability. The CMM output the parallelism as well as a calculated perpendicular distance between the two fitted planes. Δh shown in Figure 4.3 represents this measured perpendicular distance. The measurement represents the true step size from the reference plane to the top part.

The CMM measures the perpendicular distance between two parallel planes as the distance between the centroid of the datum plane and the centroid of that target plane [25]. It also outputs a value of parallelism between the two planes calculated by establishing the datum plane as a reference and drawing two planes perfectly parallel to the datum that encompass all probed points of the target plane as shown in Figure 4.3. The distance between these parallel boundary planes is set as the parallelism.

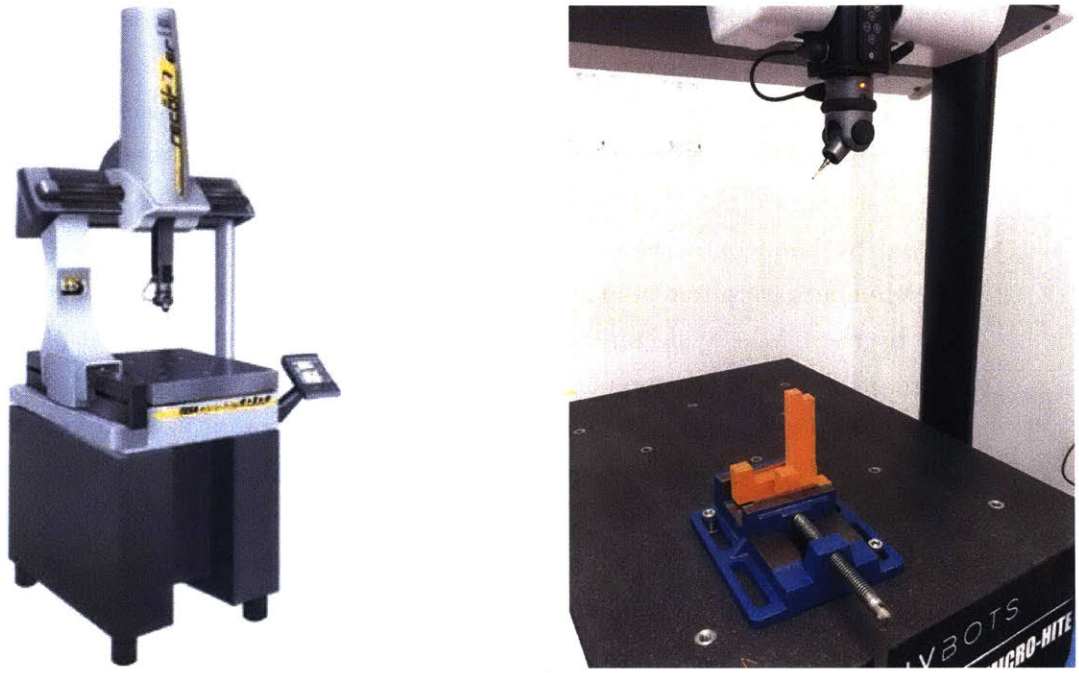

(a) TESA 3D CMM [26] (b) Mounted part view

Figure 4.2: CMM apparatus and measurement setup

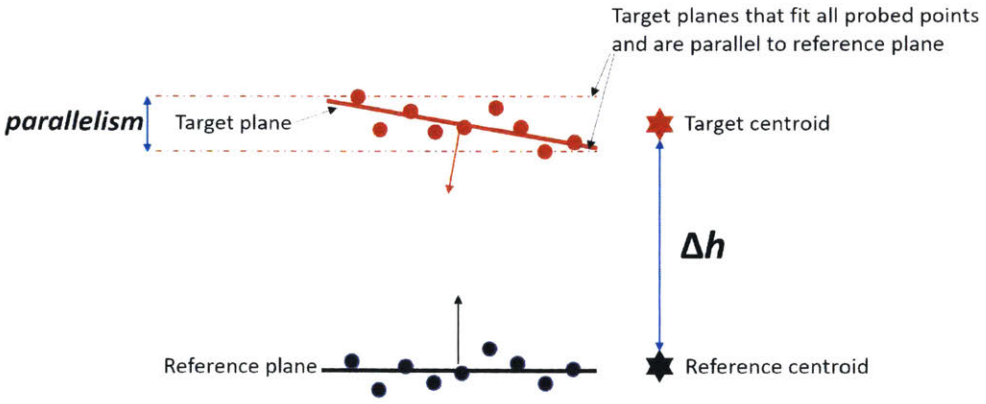

Figure 4.3: Schematic showing the measurement approach undertaken by the CMM to provide a perpendicular distance and a parallelism between two planes

4.3 Results and Analysis

4.3.1 Layer Thickness Calculation

In order to calculate the error in layer thickness, an extra step was taken to calculate the average thickness of a layer contained within the measured step size. By taking the perpendicular distance between the reference plane and the top plane and dividing it by the nominal number of layers (n) output by the G-code, the average layer thickness can be found at that build height over the given step size. This number can then be subtracted from the nominal layer thickness, given by the slicer configuration, to arrive at the average LTE. The calculation is shown below. $\bar{t}$ refers to the average layer thickness across the step size and t_{nom} refers to the nominal layer thickness provided by the slicer configuration.

$$\bar{t} = \frac{\Delta h}{n}$$

$$\Delta \bar{t} = \bar{t} - t_{nom}$$

4.3.2 Initial Measurement Method

Cleaning the Data

Having measured each part three times, the maximum difference between the measurements for each part number was plotted. This indicated the variance introduced by the measurement method. The data was filtered by removing parts from the data set that had maximum differences greater than 100 microns. Parts numbered 36, 61, 62, and 65 were removed as shown in Figure 4.4, as a consequence of severely poorer surface finishes than other parts in the data set. Number 36 also had uneven top and references planes due to the 5% infill structure used to print it.

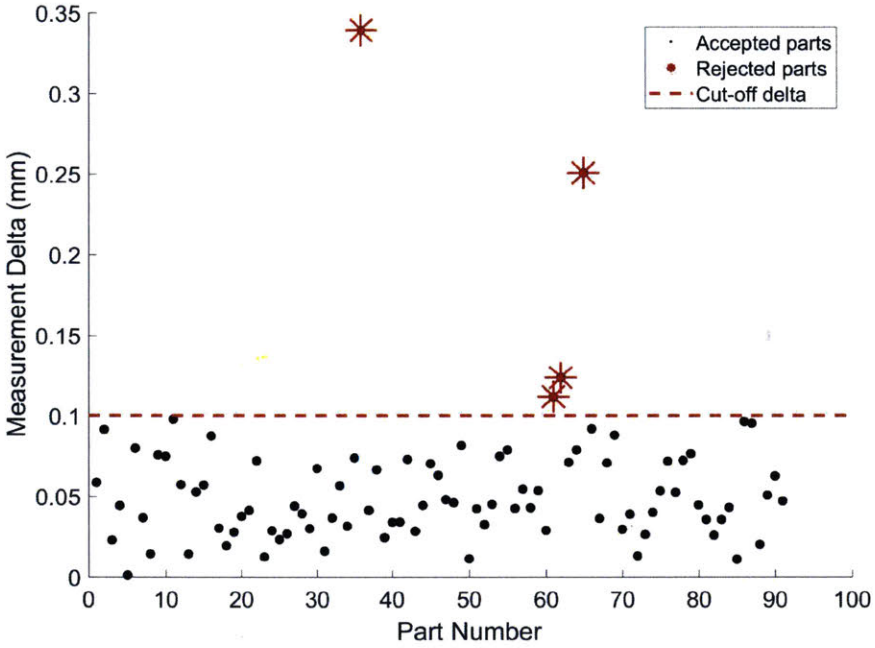

Figure 4.4: Maximum measurement difference between measurements for each part

Initial Findings

Having measured the prints from the various designed experiments and calculated the layer thickness offset from the nominal thickness, parameter effects were tested against thickness variation. Interaction effects between infill and build height were tested for standard quality parts, and for differently infill structured fast quality parts.

For standard quality parts, the per layer thickness error was not deemed to be significantly affected by either infill density or build height; thus a constant layer thickness offset was deemed to be the appropriate modeling of the data. This resulted in an average LTE of less than 0.1 microns below the nominal of $0.2mm$. This proportionally small error shows that the printer

is accurate and centered around the nominally expected layer thickness for standard quality printed parts. On the contrary, the precision of the machine remains low as parts in standard quality varied in average layer thickness from +2 microns to -2 microns, as can be seen from Figure 4.5. Since the LTE was centered around zero with very small upper and lower bounds, the total height of standard parts is often highly accurate to that which is nominally expected.

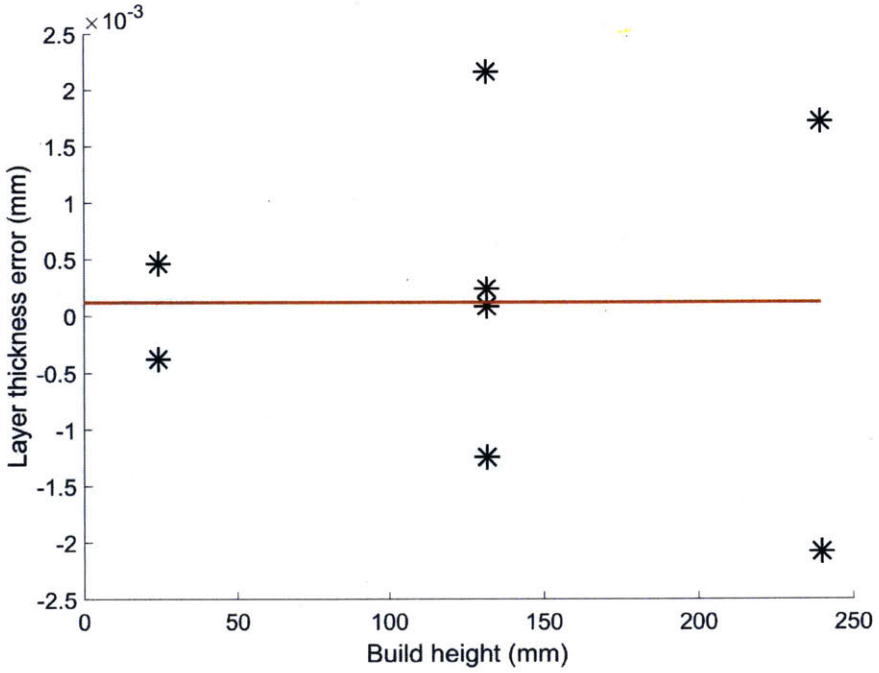

Figure 4.5: LTE for standard quality parts with mean error line

Infill Structure Inconsistencies

Having measured and qualitatively investigated non-honeycomb infill structure parts, it was concluded, due to the inconsistencies in print quality along with the lack of costumers who print in non-default structure setting (default

is honeycomb), that these parts would be removed from future analysis. The infill structures investigated are shown in Figure 4.6. As can be seen from the Figure, the 5% concentric infill structured part has no visible infill due to the slicer configurations of such a setting. This of course leads to inconsistencies when bridging material from one edge of the shell to the other. The material sinks and creates a surface greatly lacking flatness. For this and other reasons these parts were rejected.

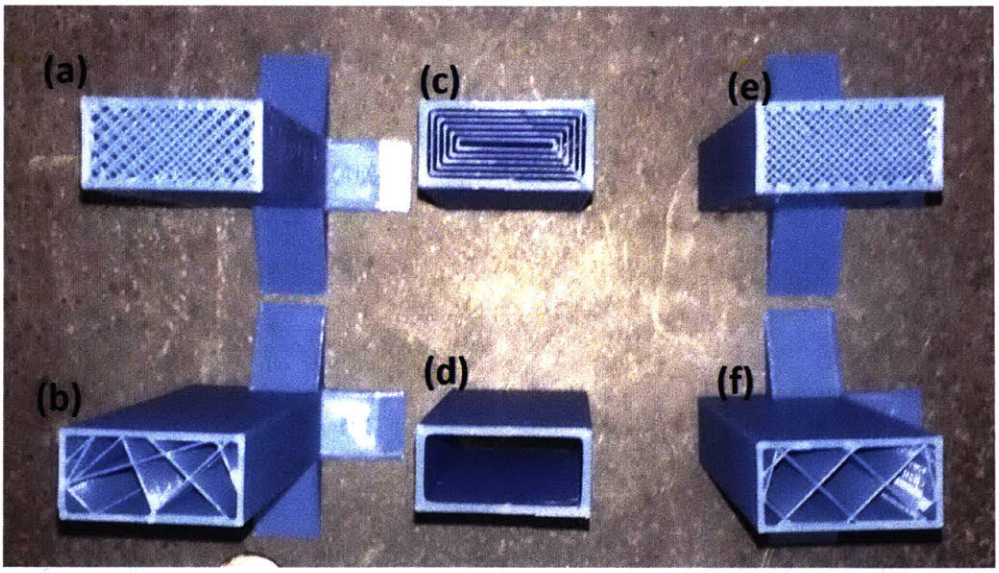

Figure 4.6: Cross sectional view of infill structures (left to right): Linear infill structure of 35% (a) and 5% (b), Concentric infill structure 35% (c) and 5% (d), Rectilinear infill structure 35% (e) and 5% (f)

Model Fitting

Model fitting was performed on the LTE versus the build height of the target plane for the remaining parts. The constant and linear models are shown in Figure 4.7 with 95% confidence intervals (CI) and their residuals. The linear model shows a negative relationship between LTE and build height.

Therefore, as the part height is increased, the LTE at taller build heights increases suggesting a cumulative error in layer thickness as the part is being built. This model was not accepted due to its insignificant build height effect p-value of 0.1 [12], as well as the lack of consistency in magnitude of fitted residuals across the build height. The constant model provides a much more significant p-value and provides a mean layer thickness offset error of -2.78 microns.

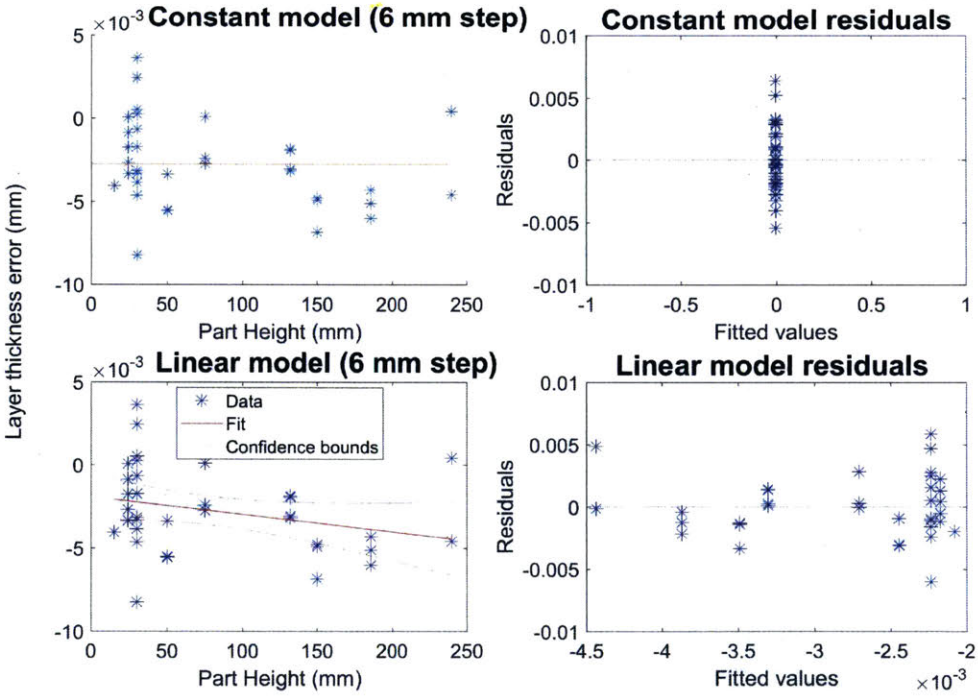

Figure 4.7: Constant and linear model fitting of LTE vs. build height for 6 mm step size

Due to previous experimentation that showed evidence of curvature between LTE and build height, the quadratic regression was tested against the data. The tested regression equation, where $\Delta\bar{t}$ refers to the average LTE across

the $6mm$ step at nominal build height H is:

$$\Delta\bar{t} = C_0 + C_1 H + C_2 H^2$$

The p-values, of the intercept and of the linear and quadratic build height effects, were once again highly insignificant. These results were then used to extrapolate a total part error at various build heights and compare the data to the part height error data collected through the NVBOTS' PAE study.

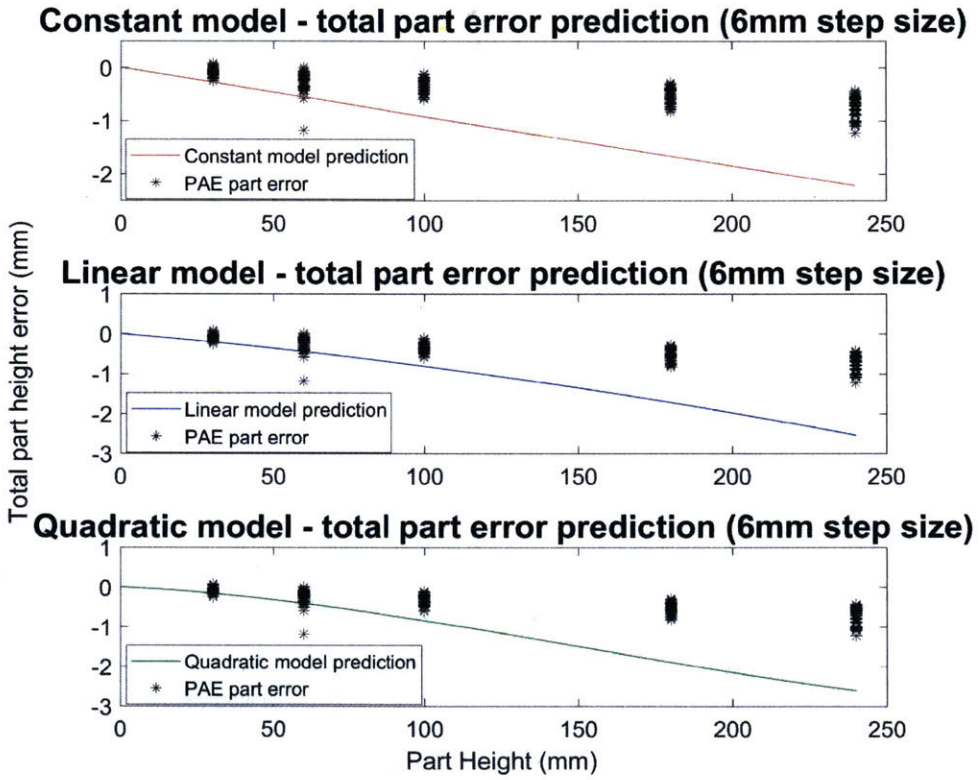

Figure 4.8: Total part height error prediction for the constant, linear, and quadratic models fitted to the 6mm step size data and overlayed by the total part error data from the PAE

From Figure 4.8 it can be seen that all three models largely over predict

the negative error in total part height. Even the highly significant constant model over predicts the error by a factor of three times at the $240mm$ part height. This prompted an investigation into the reason for the lack of consistency between the predicted and actual part height error. It was hypothesized that the small $6mm$ step size resulted in a low signal-to-noise ratio resulting from a lack of parallelism between the reference and top planes that were probed by the CMM.

Increased Step Size Model Fitting

To test the above hypothesis, parts at various build heights were designed and printed with an $18mm$ nominal step size between the top and reference planes. The parts were also redesigned to include a $5.1mm$ base step to allow for total part height measurements that would be compared to the PAE data. This would help identify whether inconsistencies occur between the two experiments thus explaining the over prediction in total height error. Fifteen parts across three different build heights that covered the entire build envelope were printed and measured. Similarly to the $6mm$ step size analysis, constant, linear, and quadratic models were fitted to the calculated LTE as a function of build height. Figure 4.9 shows the results of the constant and linear regressions. Despite a p-value of 0.0037 showing linear significance between thickness error and build height, it is evident from the scatter and fitted residuals of both the constant and linear model that some polynomial relationship exists.

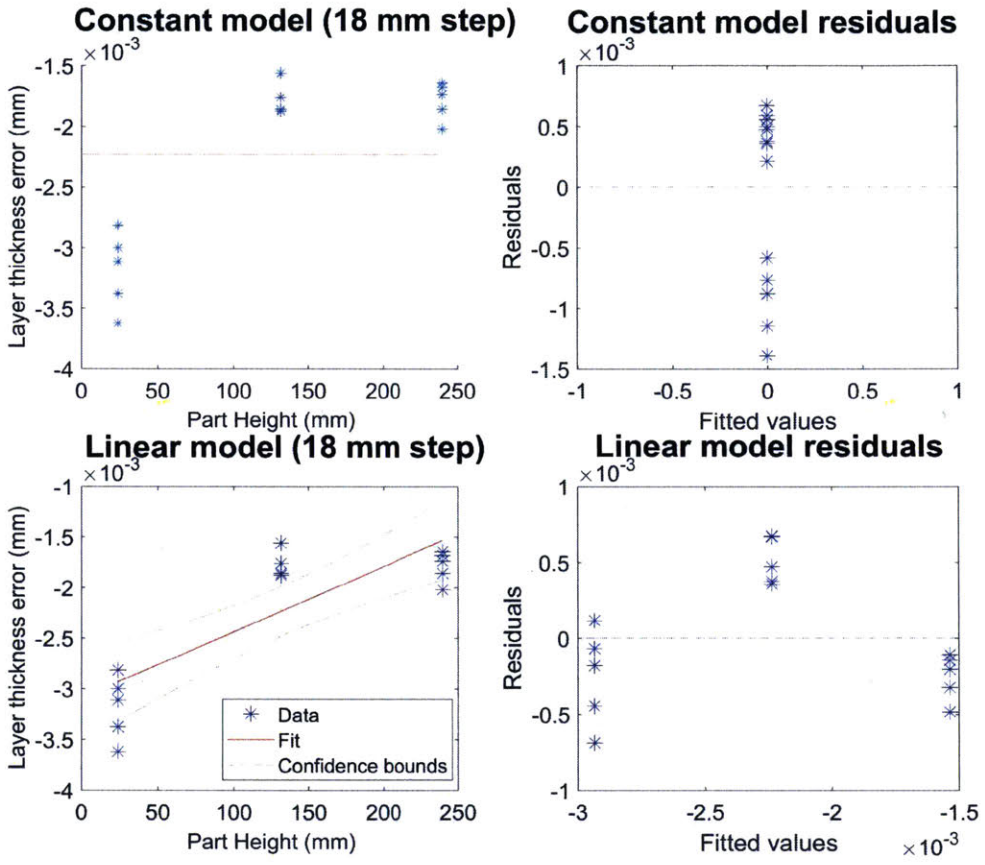

Figure 4.9: Constant and linear model fitting of LTE vs. build height for 18 mm step size

The quadratic regression to the data resulted in p-values of 7.1e-12, 2.3e-06 and 4.1e-05 for the intercept, linear, and quadratic term respectively. The R-squared of the fit was also greater at a value of 0.92. This provides very strong evidence for a potential quadratic relationship despite the lack of a large number of prints at the $18mm$ step size. Figure 4.10 illustrates the quadratic model.

Given these results, the total error was extrapolated for each model to compare with both the PAE total part height error and the total part height

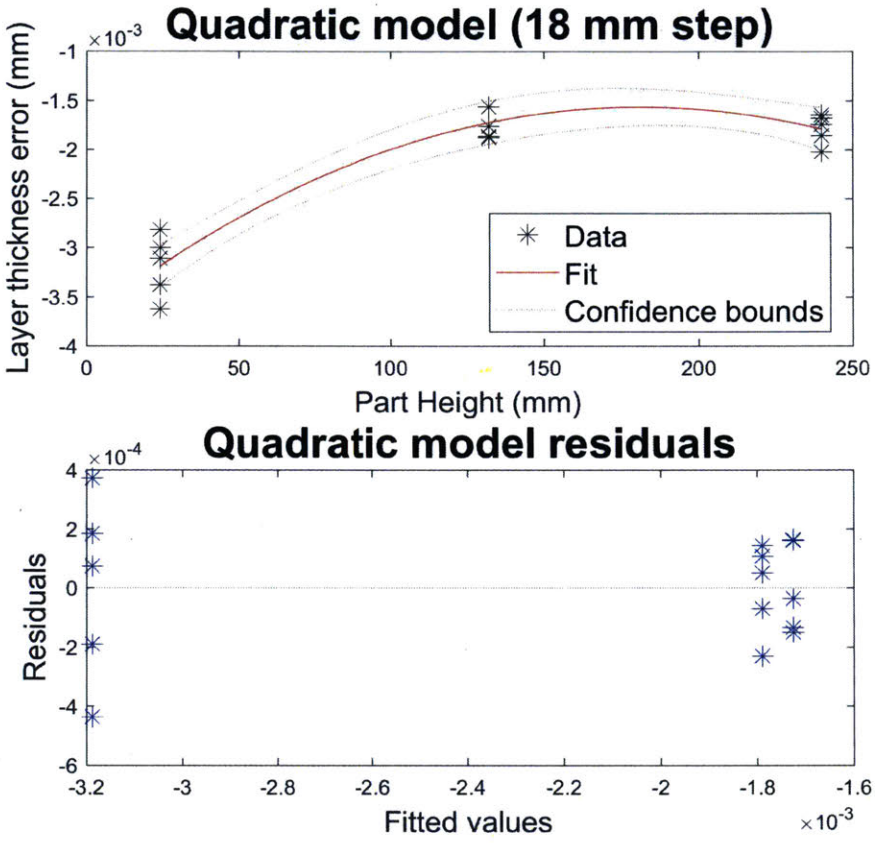

Figure 4.10: Quadratic model fitting of LTE vs. build height for 18 mm step size

error of the newly designed parts.

From Figure 4.11 it can be observed that the increased step size has more closely lined up the predicted model to both the PAE data and the new part height error data. The actual total height error of the two different data sets line up almost perfectly thus proving that total height errors have remained consistent between the time line of the PAE and this experiment. It once again proves that the error prediction model has overshot the actual data

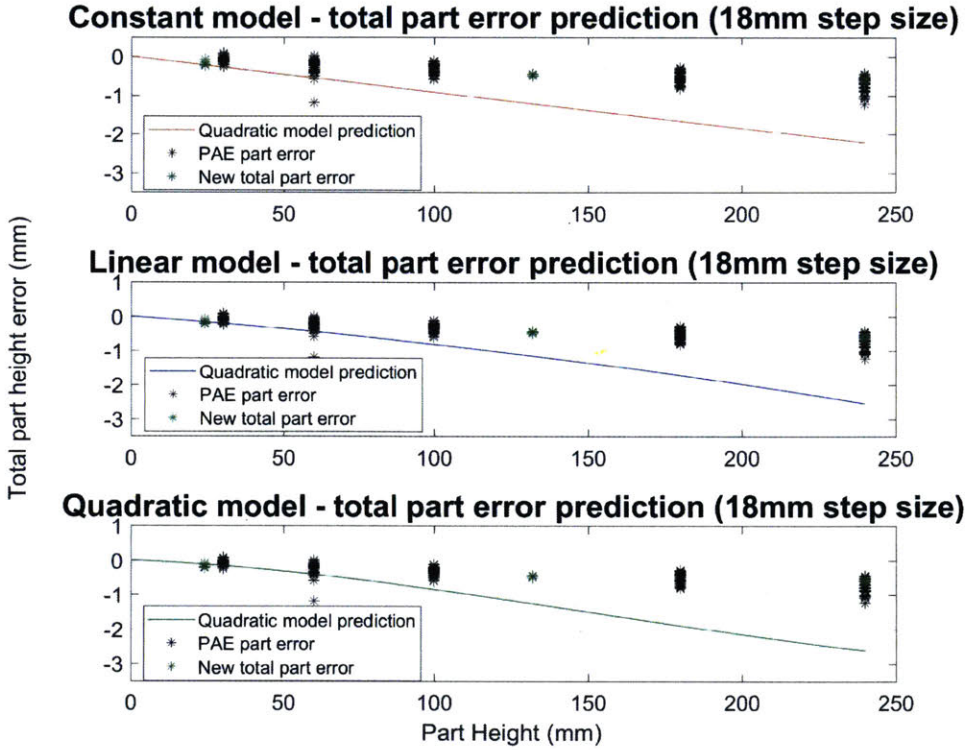

Figure 4.11: Total part height error prediction for the constant, linear, and quadratic models fitted to the 18mm step size data and overlayed by the total part error data from the PAE and the newly printed parts

and that inconsistencies still exist in the LTE approach.

4.3.3 Improved Measurement Method

New Measurement Methodology

Due to inconsistencies between the results of different step sizes, it was hypothesized that the lack of parallelism between the reference plane and the top plane provided too great of a noise to the data which yielded inaccurate results. Though an increase in step size from $6mm$ to $18mm$ decreased the factor of inaccuracy, the inconsistency was still evident. In order to attempt to mitigate the noise, a new measurement method was introduced. The reference plane was measured on the newly included base step of $5.1mm$ for PLA parts using the same CMM approach (H_{ref} in Figure 4.12). This distance was then subtracted from the perpendicular distance measured from the base step to the top plane (H_{total} in Figure 4.12) thus yielding a new true step size. This approach proved to be more reliable and repeatable across parts. The adjusted layer thickness calculation is shown below:

$$\Delta h = H_{total} - H_{ref}$$
$$t = \frac{\Delta h}{n}$$
$$\Delta t = t - t_{nom}$$

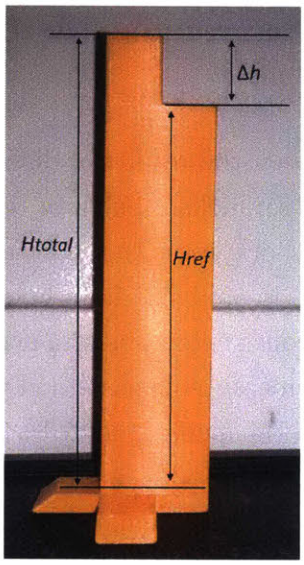

Figure 4.12: Perpendicular distance of step schematic

Gage R&R Study

Having remeasured the $18mm$ step sized parts using the improved method and repeated the method three times for each part, a Gage repeatability and reproducability study was performed to verify the measurement method's capability. Gaging the measurement of H_{total} as shown in 4.12 resulted in a percent of Gage R&R of total variations less than 1%. This concluded that the measurement method is capable of reproducing the results.

Model Fitting

Given the results of the Gage R&R study, all fifteen $18mm$ step sized parts were plotted and fitted with constant, linear, and quadratic models. Once again, similarly to the the original results arrived at from these $18mm$ step size parts, the constant and linear models were determined as inaccurate due to the plotted residuals in Figure 4.13. These residuals provided evidence to some higher order relationship between LTE and build height. The quadratic

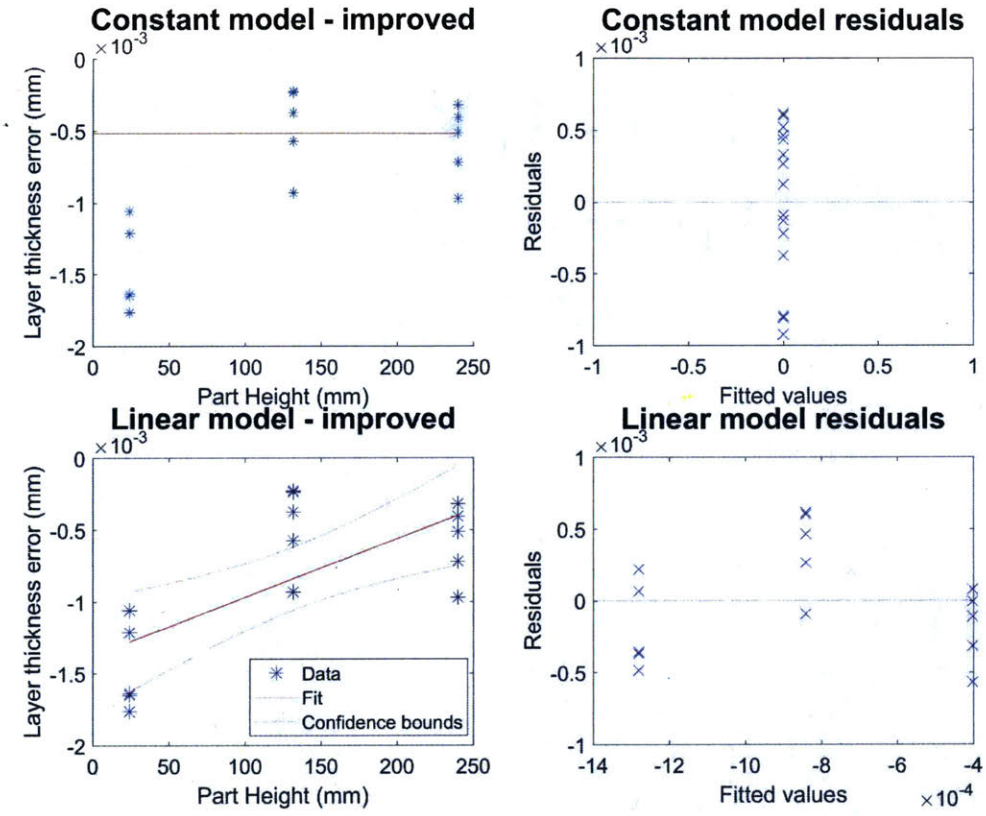

Figure 4.13: Constant and linear model fitting of LTE vs. build height for 18mm step size using improved measurement method

regression of LTE versus build height provided highly significant p-values for the intercept, linear, and quadratic terms (4.3e-07, 6.8e-04, and 4.2e-03 respectively) with an R-squared of 0.75. Once again, a potential quadratic relationship fit is strongly supported by the regressions results. Taking all three models, total part height errors were extrapolated and compared to the PAE data as well as the new part height errors calculated from the H_{total} measurement. As can be seen from Figure 4.14, the predictions line up almost perfectly to both the PAE and new part error data. The magnitudes of total part height error across the whole z-axis build envelope are comparable. This

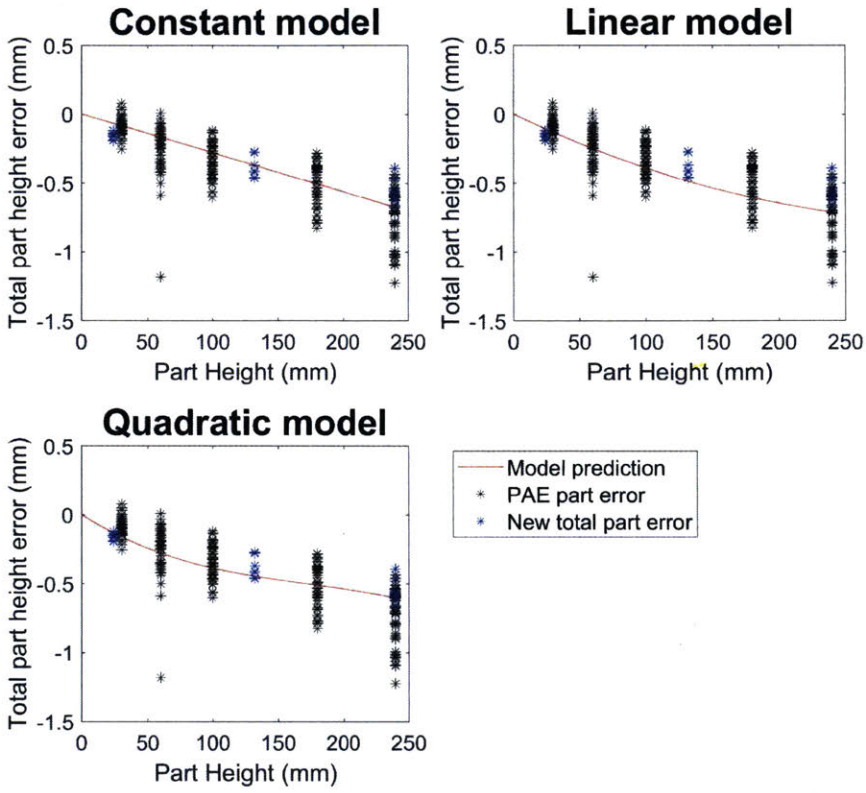

Figure 4.14: Total part height error prediction for the constant, linear, and quadratic models fitted to the $18mm$ step size data and overlayed by the total part error data from the PAE and the newly printed parts using the improved measurement method

shows great improvement in part measurement accuracy when using the new methodology.

Prediction Intervals (PI) Implementation

In order to determine the sensitivity of the predicted total part height error using the quadratic model, prediction intervals were calculated and trans-

formed to fit the predicted total error model. Prediction intervals provide the limits of future predicted values from a model given a new model input value to a specific confidence level. In order to calculate 95% prediction intervals for the quadratic model across the build height enevelope, the following equation was used [27]:

$$\hat{t}_h \pm t_{a/2,n-2} * \sqrt{MSE(1 + \frac{1}{n} + \frac{(H_j - \bar{H})^2}{\sum (H_i - \bar{H})^2})}$$

This calculation provided prediction intervals plotted over the model in Figure 4.15. These intervals explain that, to 95% confidence, any future calculated LTE should fall within the black bounds [1].

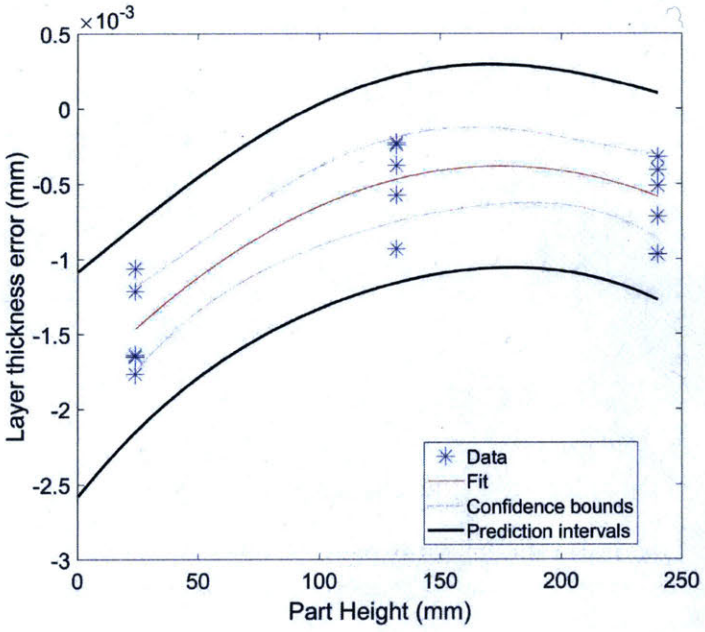

Figure 4.15: Quadratic model fitting of LTE vs. build height for 18 mm step size parts with 95% Confidence Intervals (CI) and PI, using the improved measurement method

[1]The MATLAB function used to calculate the PI is explained in [28]

Given the calculated PI presented in Figure 4.15, Figure 4.16 shows the predicted total part height error with 95% PI, extrapolated from the quadratic LTE model, and compared to PAE and new part height errors. It can be seen that the 95% PI do a good job of capturing the noise associated with printed parts from the PAE data. A large majority of the points fall within the bounds, especially at build heights greater than $50mm$.

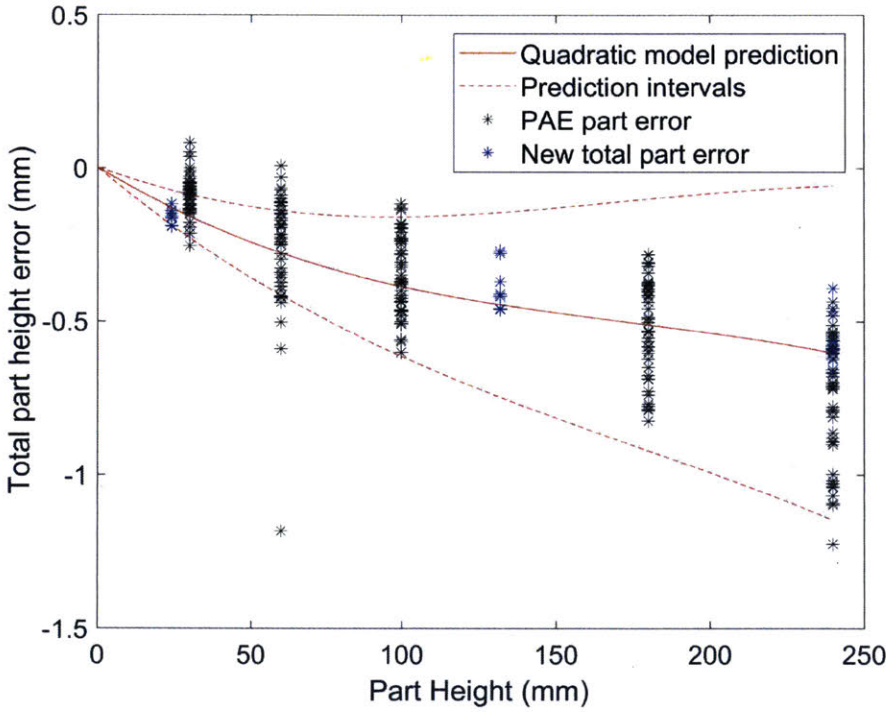

Figure 4.16: Quadratic model total part height error prediction with 95% PI, using the improved measurement method, overlaid by PAE and new part error

Chapter 5

Modeled Compensation

5.1 Compensation Method

In order to utilize and test the validity of the quadratic LTE model, the total part height error prediction can be used to add compensation to the part. With the modeled compensation, the accuracy of the printed parts should increase. The G-code level compensation implementation method used is outlined in Lee's thesis [2]. The compensation script "acts on an uncompensated G-code file produced by a slicer package and a CSV file containing error model coefficients and produces a new G-code file with compensation applied" [2]

For an NVPro to print a part, it requires firmware-level instructions found in a G-code file. G-code files contain code that describes each linear movement of the printer head by assigning starting and ending x and y coordinates. The code also includes instructions for extrusion and retraction points as well as filament extrusion speed used during extrusion. The G-code also sends print bed z-positioning commands. These commands are interpreted sequentially and executed by the printer. The compensation method proposed on Lee's thesis relies on adjusting the G-code generated from the sliced STL part file through implementation of a polynomial compensation model. Since the

LTE approach solely focuses on part height effects on thickness error, the compensation to G-code is only applied in the z-dimensional print bed positioning. The print bed is commanded to adjust from its nominal layer thickness movements in order to compensate for the error. The number of layers is kept consistent to the originally sliced part, but the nominal layer thickness is constantly being adjusted during the part build.

5.2 Compensation Results

To verify that the total part height error model works, 15 columns were printed using post-compensation G-code. These 15 parts were spread across 5 build heights and their total height was measured and compared to the expected height. The results of the compensation are shown in Figure 5.1. The histogram shows the total part height error in millimeters and its occurrences in the PAE study as well as the error and occurrences for the compensated parts. Though the sample set of compensated parts is significantly smaller than that of the PAE study, it can clearly be seen that the compensation has improved the accuracy of the printer in the z-dimension. The compensated parts have an error centered around $0mm$ with a maximum height error of 130 microns above the nominal height. It also seems that the precision of the printer has been increased simultaneously and unexpectedly. The range of errors is 190 microns across all part heights. The pre-compensated part height errors ranged from $-1.2mm$ to $+0.08mm$. But again, this can not be fully confirmed due to the small sample size of measured compensated columns.

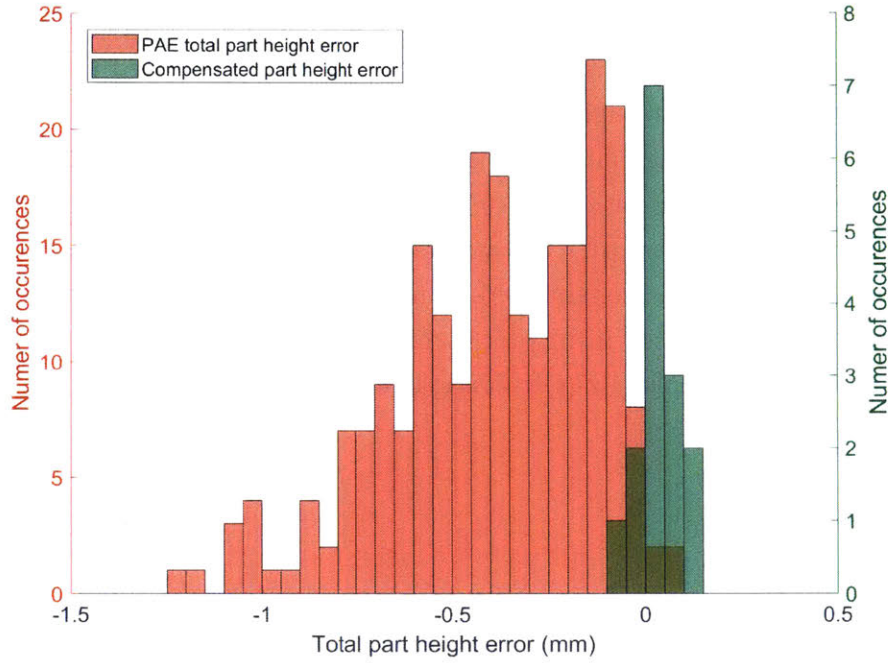

Figure 5.1: Total part height error comparison between PAE parts and newly printed compensated parts

5.3 Possible Explanations for Height Inaccuracies

Having successfully compensated for height inaccuracies of PLA parts and comparing the results with Lee's experiment [2] it is evident that a constant height accuracy error exists for PLA parts being printed on the NVPro. One of the hypothesized reasons behind these inaccuracies was the shrinkage caused by the elastic and viscoelastic effects of PLA fused deposition discussed in the paper by Costa et al. [17]. A second hypothesis was that the print bed was not exactly at its nominal z-dimensional position when instructed through the G-code. This would cause a larger or smaller gap be-

tween nozzle and print surface, thus causing error in layer deposition. This hypotheses was quickly tested using a dial gauge. The dial gauge was fastened against the frame of the printer. The print bed was commanded through G-code inputs to move to different z coordinates allowed to move to different heights. The dial gauge measured the change in z axis position of the print bed from the zeroed position. Just by performing a few preliminary test, it was confirmed that the print bed was rarely found precisely at the nominal height at which it was commanded. Further similar positional tests with a more repeatable measurement process could confirm and quantify the error associated with print bed z-positioning inaccuracy.

Chapter 6

Acrylonitrile Butadiene Styrene (ABS+) Experiment

6.1 Goal of Experiment

The goal of the ABS+ experiment is to model the overall part height deviation by taking layer-to-layer thickness deviation across the part's build height and various infill densities. Because only a single, reliable slicer configuration exists for ABS+ printed parts, no print quality effects were tested. Since the ABS+ parts were printed on the HT version of the NVPro, this experiment could provide insight regarding printer to printer variation. It also serves as data comparison to the PLA results to test whether material variations in LTE's exist. The measurement method used was the improved method explained in Section 4.3.3 due to its repeatability, reproducability, and higher accuracy.

6.2 Design of Experiments

The initial experiment was designed to test the effect of build height on LTE and to examine the possibility of curvature, similarly to the PLA data. Since

the FDM process remains noisy, and the ABS+ part reliability is lower than that of PLA, a 2^1 experiment with 3 replicates and 6 center points was used. Table 6.1 outlines the amount of parts and their heights printed at each level.

Table 6.1: Full DOE for ABS+ LTE vs. build height

Level	Build Height	Number of parts
+1	239.91mm	3
-1	15.12mm	3
CP	150.16mm	6

Because of certain part quality inconsistencies discussed below, extra parts were printed at heights less than 150mm in order to negate the effects of noise from lack of quality. Six parts at three different heights were also printed with 25% infill density to test the effect it has on LTE.

6.2.1 Adjusted Test Part Design

The reliable slicer configuration of ABS+ most closely represents the configuration for standard quality PLA parts in relation to the nominal layer thickness and the initial layer offset. For ABS+, the nominal target layer thickness is $0.212mm$. In order to achieve an integer number for number of layers in the total part and in the step the test part design had to be adjusted for each height targeting a different level in the print envelope. The step size was changed to $4.23mm$ so that it can incorporate 20 layers nominally [1]. The base plane of the part was changed to $2.96mm$ and the total part heights were rounded to the closest layer thickness.

[1] 20 layers was the nominal step size target for $6mm$ PLA fast quality parts

6.3 Results and Analysis

6.3.1 Layer Thickness Error Modeling

An initial glance at the scatter of LTE versus build height shown in Figure 6.1 shows wide variation in LTE for taller parts. This is primarily caused by lack of part quality, which is discussed later in this chapter. Trying to fit constant, linear, and quadratic models to the data as is, provides insignificant p-values and low R-squares. After consultation with the NVBOTS' engineering team, it was decided that the $240mm$ parts would not be considered for future model fitting because of their high variability.

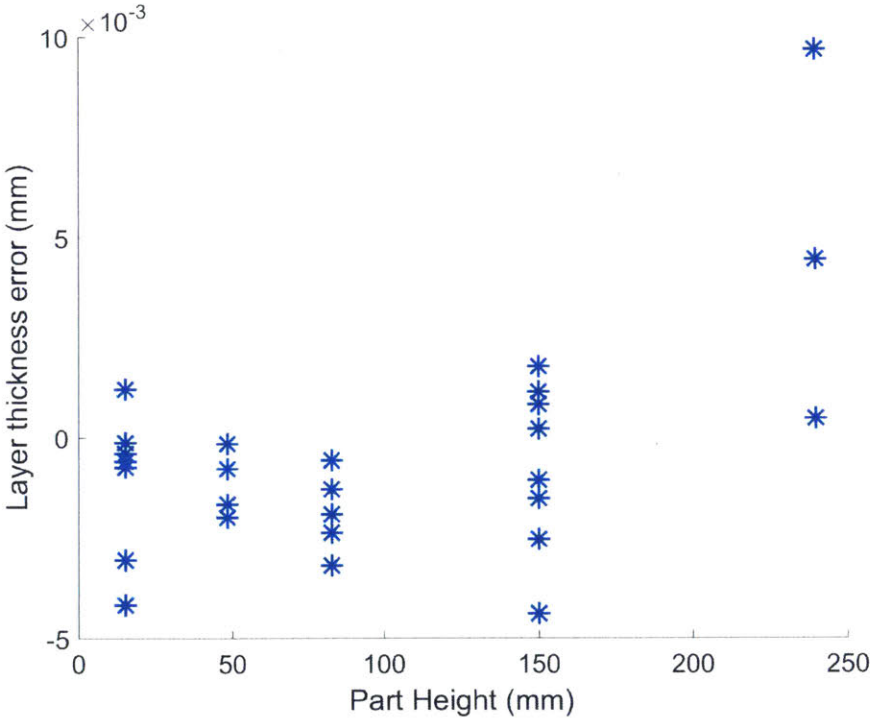

Figure 6.1: All ABS part LTE plotted against the part height

Having removed the $240mm$ parts, all three models were fitted to the

data and compared. From the regression results it is evident that the inconsistencies and noise involved with printing ABS were creating linear and quadratic relationships that seemed unreasonable. The best course of action was to derive a constant LTE across the whole build height of the part and use that constant offset to generate a total part error compensation model. The scattered data (without the $240mm$ parts), along with the mean fit, is plotted in Figure 6.2.

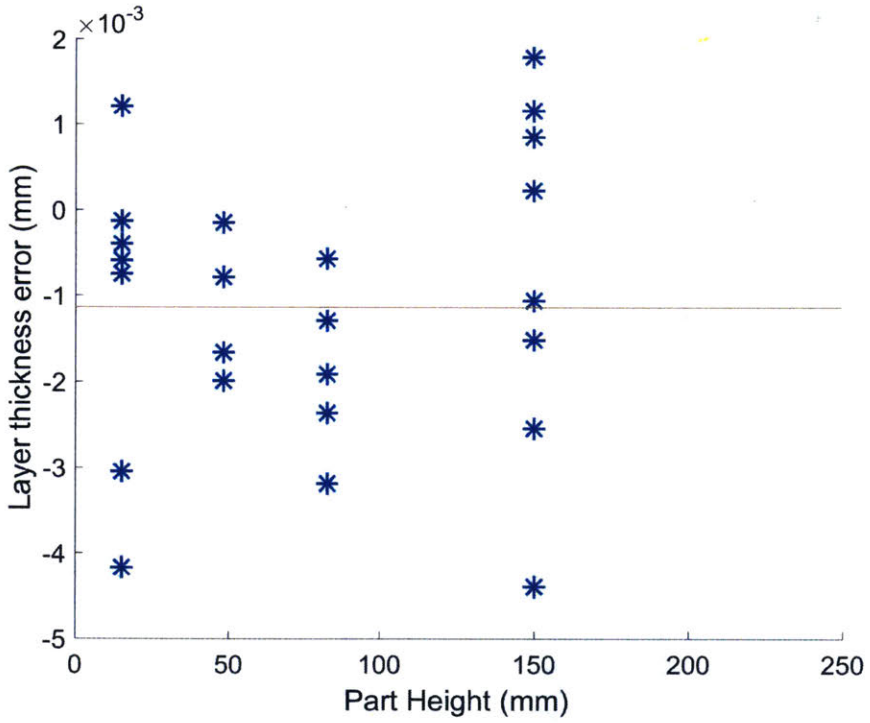

Figure 6.2: ABS LTE constant modeling with removed 240mm parts

The constant thickness error from this data is estimated to be around -1 microns per layer.

6.3.2 Cumulative Part Height Error

Using the constant LTE, a compensation model was extrapolated. This of course resulted in a negative linear relationship for LTE as a function of build height. The resulting model was plotted and compared with total part height error in Figure 6.3. Total part height error was once again calculated by measuring the H_{total} between the base and top planes and subtracting the nominal height from it.

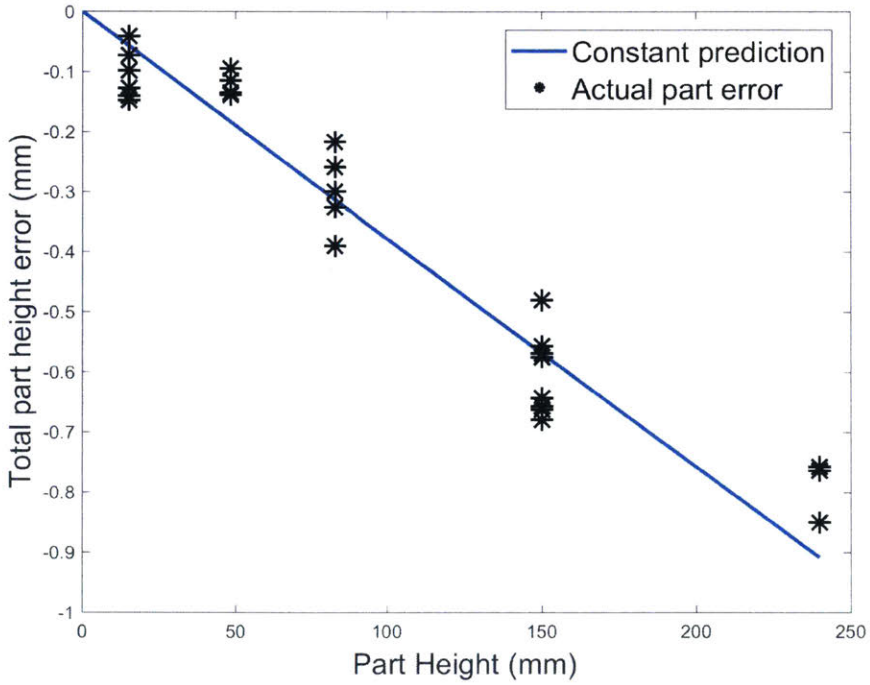

Figure 6.3: ABS total part height error prediction model using constant layer thickness model and compared to actual part height errors

The prediction model lines up well with the actual error data. The only significant deviation between the model and the actual data exists at $240mm$ height parts were quality inconsistencies, once again, play a major factor.

6.3.3 Part Quality Inconsistencies

The current quality of printed ABS+ parts is inconsistent and the slicer configuration for these parts is not yet optimal. This causes parts to print with multiple defects. The most common quality issues that arise with printing tall parts are shown in Figures 6.4a and 6.4b. Gaps formed between layers as adhesion between the material failed. Other instances demonstrated over-extrusion of ABS+ causing the layers to widen in the x and y directions. The

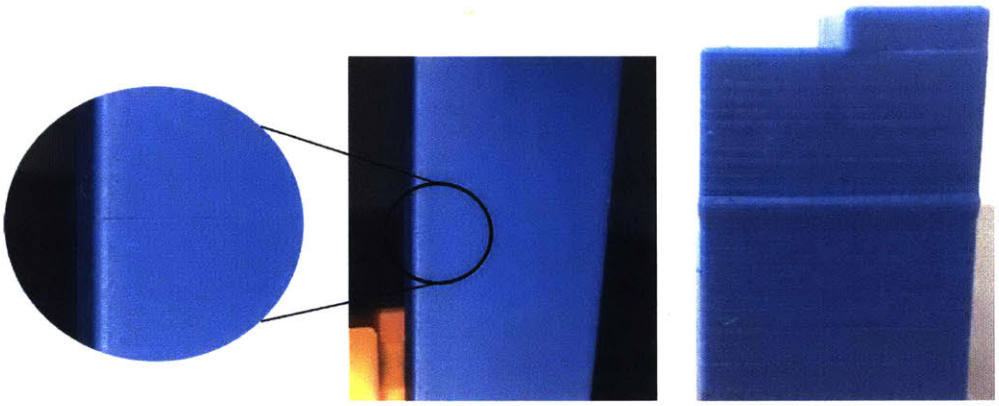

(a) Adhesion gaps between layers (b) Over-extruded layers

Figure 6.4: Most common ABS+ part quality defects observed that affected the reliability of LTE results

presence of gaps between layers weakens the parts and makes them prone to cracking. They can easily be damaged by over tightening the clamp used to fix the parts on the CMM bed.

6.4 Material Comparison

In order to test for consistency across the two materials, an analysis of covariance (ANOVACOVA) was performed on the linear models fitted to the total part height error of ABS+ and PLA. The MATLAB results of the analysis

of covariance are shown in Figure 6.5 and Figure 6.6. The interaction term between material and build height has an F statistic of 32.54 and p-value of 0 thus concluding that the slopes of the two materials are significantly different [29].

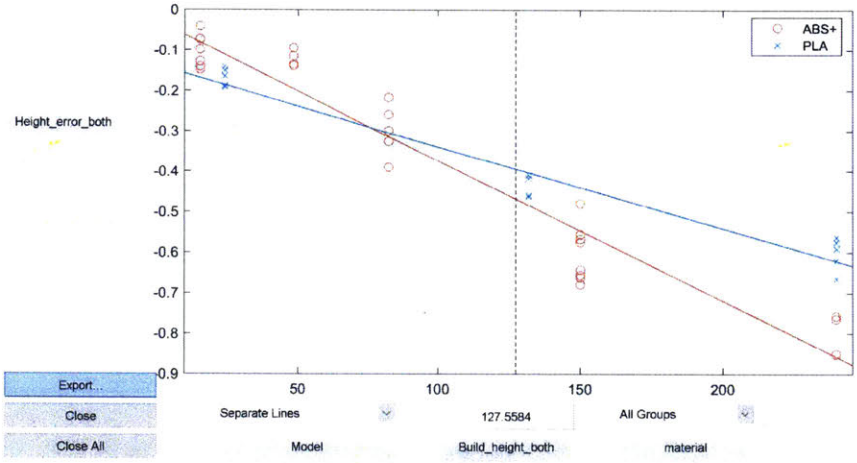

Figure 6.5: Analysis of covariance data set plot comparing the total part height error as a function of build height for PLA and ABS+

A test was also run to test the significance of constrained slope through the two data sets. The slope was constrained so as to provide two parallel lines that fit through both the PLA and ABS+ data. The test resulted in insignificant slope coefficients for both data sets, providing further evidence that the relationships of total part height errors across build height for the two materials are statistically different. These results are once again not fully conclusive due to the current lack of quality in ABS+ printed parts that may have skewed the data.

PLA comparisons between the NVPro and NVPro HT were not conducted due to time constraints and lack of reliability when it came to printing PLA parts on the NVPro HT.

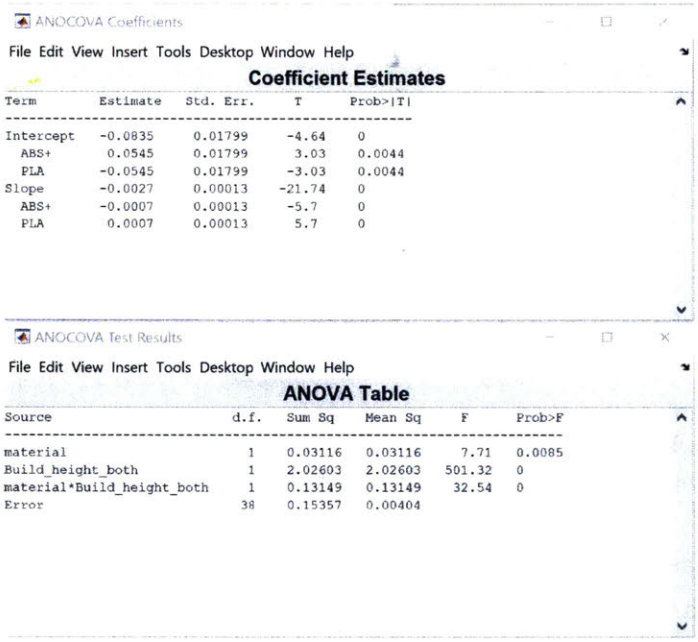

Figure 6.6: Analysis of covariance coefficients comparing the total part height error as a function of build height for PLA and ABS+

Chapter 7

Conclusion

This thesis explores a layer by layer thickness error modeling approach to explain total part errors in the z-direction. The approach has been tested across various build heights, infill densities, print qualities, and print materials. Using the improved height measurement methodology outlined in Section 4.3.3, the layer thickness error model was able to accurately predict the total part height error of PLA columns of different densities and heights.

An extrapolated error compensation model was implemented using G-code modification and the parts were tested. Preliminary results show an increase in accuracy which has centered total part height error around $0mm$. Precision and repeatability of the printer seem to have also improved through the implementation of the compensation model.

ABS+ parts were also designed and measured in the same fashion as PLA. Results from this experiment seemed less conclusive as the quality of the printing was not consistent across the whole batch of parts. A similar total part height error trend exists in ABS+ as in PLA. Total part height error increases significantly as the part build height is increased.

The proposed layer thickness approach yields dependable results for PLA parts and can be easily implemented to a variety of FDM printers and print materials that have consistent print qualities. Apart from providing an in-

sight into the effect of printer and part parameters on the z-dimensional accuracy of a part, this work also contributes an experimental methodology that can be generalized and applied to various FDM printers that use altering print settings and print materials. The LTE approach experiment is reliable and can be implemented into NVBOTS' NVPro and NVPro HT quality control (QC) procedure.

Chapter 8

Recommendations and Future Work

8.1 Confirming Predictive Relationship

All three PLA prediction models are plotted in Figure 8.1 for comparison. The differences among the three extrapolated models are not clearly discernible and thus further part printing and measuring at various heights can be performed to formulate stronger and more robust evidence for why the LTE has a quadratic relationship to build height. By printing more $18mm$ step sized parts all along the build height, a more distinct model can be developed and tested.

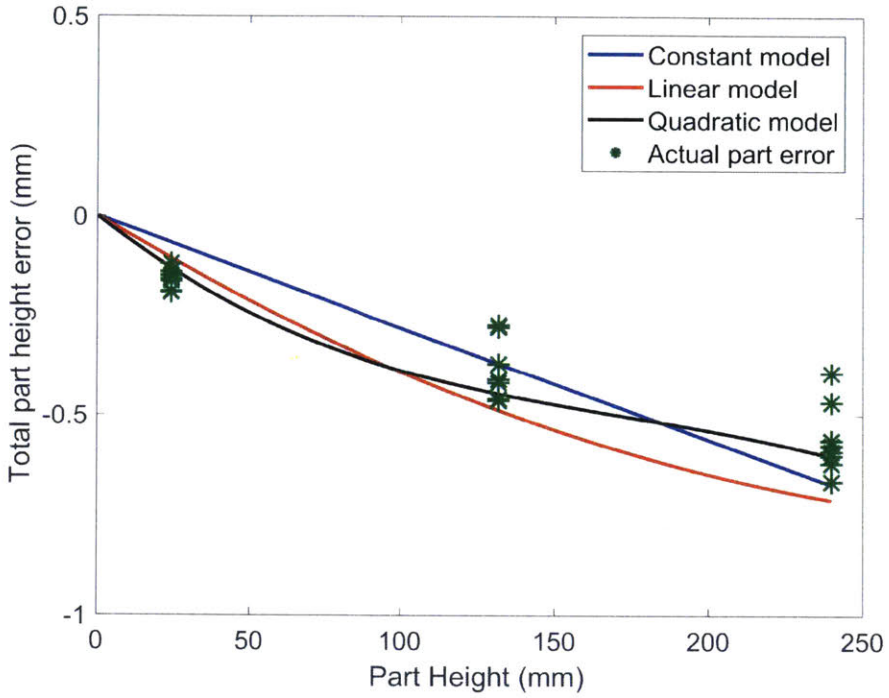

Figure 8.1: Exrapolated total part height error from the constant, linear, and quadratic models overlayed by the new total part height error data

8.2 Suggested Quality Control Procedure

This section details a suggested QC procedure that can be implemented during the final testing of the printers coming off the line. This procedure will allow for performance of similar testing and analysis, detailed in Chapters 4 and 5, on various NVPro and NVPro HT printers, as well as on newly qualified and reliable print materials.

8.2.1 NVPro PLA Quality Control

The suggested QC approach for measuring the accuracy of new printers printing in PLA, involves the printing and measuring of 15 artifacts at 5 different build height levels. These artifacts will be designed with a reference base, a reference step plane, and a top plane. Table 8.1 shows the suggested PLA part height dimensions and quantities to be printed on each new NVPro.

Table 8.1: Part z-dimensions to be printed on each NVPro printer for accuracy QC and compensation implementation

Number of parts	Top plane (mm)	Step reference (mm)	Base reference (mm)
3	30	12	5.1
3	84	66	5.1
3	135	117	5.1
3	186	168	5.1
3	240	222	5.1

Once this experiment has been performed on a small sample size of printers, further analysis can be conducted to test for printer to printer variations in LTE. If the results imply that no printer variation exists, then the same compensation method can be applied and tested on all similar version printers that have had no significant hardware changes implemented.

8.2.2 NVPro HT Quality Control for New Materials

A variation of the above experiment can be performed for newly qualified materials being printed on the NVPro HT. Since there is no preexisting insight on new material inaccuracy, a fuller experiment will have to be performed. A recommendation of 30 parts printed over 5 heights is put forth for newly qualified materials. 6 parts at each height shown in Table 8.1 should be printed and measured. The total part height error model should then be extrapolated form the LTE model and compared to actual part height error

of the printed parts. Note that the actual heights of each plane will have to be adjusted to account for any new nominal layer thickness setting outputted by the optimal slicer configuration. Refer to Section 6.2.1 where this design adjustment was made for a new nominal layer thickness associated with ABS+ printing. The analysis conducted will remain consistent to that of the PLA experiment.

8.2.3 Optimizing Part Design

One of the difficulties with the experiments outlined in Chapters 4 and 6 was that the CMM measurement method was manually performed. This made measuring all these part tedious and time-consuming. A part redesign is suggested in order to be able to program the CMM to automatically measure the base, reference, and top plane of the column and output the various height measurements demanded. The CMM can be easily programmed to do so if every new part is expected to be in the same x and y position on the CMM measuring bed. The initial y position can be re-homed for every part. This would allow the CMM to automatically probe each part's plane 8 times. The revised plan is pictured in Figure 8.2. The cross base has been kept for

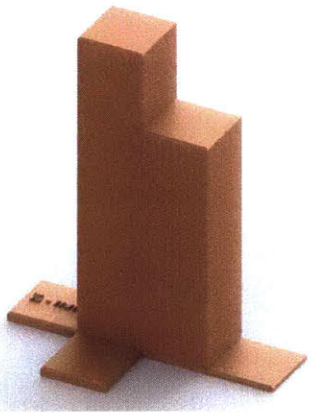

Figure 8.2: Proposed column artifact design

stability but it has been slightly elevated to avoid lining up with the reference base. This helps avoid long extrusion lines that cause defects in the surface finish of the part and thus decreasing the likelihood of measurement errors of the base plane.

8.2.4 Measurement Fixture

With the redesigned artifact picture above, a new paired measurement fixture can be designed and built to help maintain constant x and y coordinate planes when automatically measuring the part. The part drawing of the fixture can be found in the appendix. An assembly of the part and fixture is pictured in Figure 8.3. This fixture allows for repeatability of the x and y

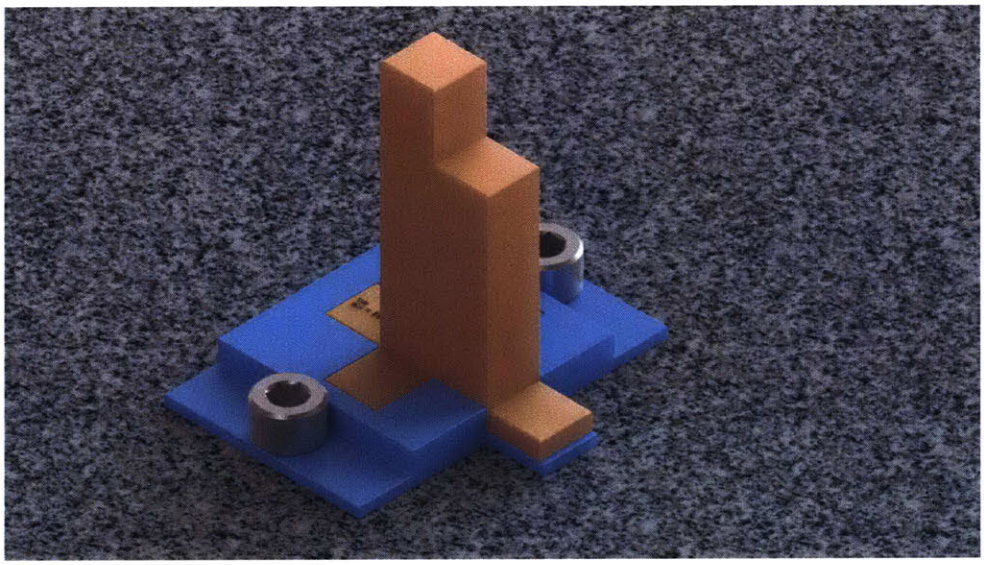

Figure 8.3: Proposed fixturing part and method for future LHE experiment

coordinates for every new part being mounted. It also utilizes the M10 bolts that fixture parts onto the CMM bed in order to maintain exact positioning of the part. This part can be 3D printed or machined out of acrylic or

aluminum. The surface finish of the fixturing part is not critical to the accuracy of the measurements.

8.2.5 Implementation

Having modeled the LTE of each machine passing through the line, a small sample of 10 compensated columns at five random heights can be printed and measured to test the validity of the compensation. The parts can be compensated using the G-code based method explained in Section 5.1. This can also be done for new material accuracy qualification on the HT printers. The compensated parts can then be measured using the new automated CMM program and part fixture. Through the measurements, the compensation model can be verified as accurate and the height compensation can be applied to all future prints of that material on that specific NVPro printer number.

8.3 Computer Vision

Throughout the length of this project, a continuous discussion between the NVBOTS engineers and the MIT MEng took place regarding the application of in-process measurement and control. Due to the lack of desire to change the hardware of the NVPro, the idea was rejected as a possible project problem solution. However it does remain as a reliable alternative to the compensation methods described in this document and in Lee's thesis.

LTE modeling can be a precursor to such a compensation approach. It has been shown that cycle-to-cycle feedback control can eliminate systematic errors of a process in steady state [21],[22]. Taking a computer vision, layer to layer approach can allow the NVPro to adjust its G-code commands to compensate for errors in part height. However, the significant investments in hardware remain a major obstacle to the implementation of such an approach.

Yet, the author maintains that such an investment in the long run should be made as cycle-to-cycle feedback control, at a layer level, can greatly increases the dimensional accuracy of the NVPro printer.

This page is intentionally left blank.

Bibliography

[1] Y. Xu, "Modeling Print Time for a Fused Deposition Modeling Machine," Master's thesis, Massachusetts Institute of Technology, Sep. 2017.

[2] S. Y. Lee, "Height Error Mapping and Compensation for a Fused Filament Fabrication Machine," Master's thesis, Massachusetts Institute of Technology, Sep. 2017.

[3] T. A. Grimm, Grimm & Associates, Inc., "Fused Deposition Modeling: A Technology Evaluation," 2002,[Online], <http://tagrimm.com/downloads/fdm-white-paper.pdf>.

[4] *3D Printing: Consumer vs Professional*, Xometry,[Online], <http://pages.xometry.com/consumer_vs_professional>, Accessed: 18 July 2017.

[5] B. Meyer, "The accuracy myth," Stratasys, Inc., Tech. Rep.

[6] *About Us/NVBOTS*, [Online], <https://nvbots.com/about/>, Accessed: 6 March 2017.

[7] *Hardware/NVPro/NVBOTS*, [Online], <https://nvbots.com/hardware/>,Accessed: 17 March 2017.

[8] *Material Developers/NVBOTS*, [Online], <https://nvbots.com/material-developers/>, Accessed: 5 July 2017.

[9] *3D printing G-code tutorial*, [Online], <https://www.simplify3d.com/support/articles/3d-printing-gcode-tutorial/>, Accessed: 18 July 2017.

[10] *Accuracy and Precision*,MATH is FUN, [Online], <https://www.mathsisfun.com/accuracy-precision.html>, Accessed: 31 July 2018.

[11] A. Chandar, "Printer accuracy experiment", Internal printer accuracy study carried out at NVBOTS, April 2017.

[12] D. Montgomery, *Introduction to Statistical Quality Control*, Wiley, 2009, 6th ed., pp 141-169.

[13] P. Gkaliamoutsas, S.-Y. Lee, and Y. Xu, "Height Accuracy in Fused Deposition Modeling: A layer-by-layer perspective",Final project for 2.830, MIT, May 2017.

[14] L. Xinhua, L. Shengpeng, L. Zhou, X. Zheng, C. Xiaohu, and W. Zhongbin, (2014, August), "An investigation on distortion of PLA thin-plate part in the FDM process", The International Journal of Advanced Manufacturing Technology, London, [Online], <https://link.springer.com/article/10.1007/s00170-015-6893-9>.

[15] T.-M. Wang, J.-T. Xi, and Y. Jin, "A model research for prototype warp deformation in the FDM process," The International Journal of Advanced Manufacturing Technology, London, April 2006, [Online], <https://link.springer.com/article/10.1007/s00170-006-0556-9>.

[16] J. Zhang, X. Z. Wang, W. W. Yu, and Y. H. Deng, "Numerical investigation of the influence of process conditions on the temperature variation in fused deposition modeling," Materials & Design 130 (2017), pp. 59-68

[17] S. F. Costa, F. M. Duarte, and J. A. Covas, "Thermal conditions affecting heat transfer in FDM/FFE: a contribution towards the numerical modelling of the process," Taylor & Francis, September 2014.

[18] A. K. Sood and R. K. Ohdar, "Grey Taguchi Method for Improving Dimensional Accuracy of FDM Process," Paper of AIMS International COnference on Value-based Management, August 2010.

[19] T. Pfeifer, C. Koch, L. V. Hulle, G. A. M. Capote, and N. Rudolph, "Optimization of the FDM Additive Manufacturing Process," University of Wisconsin, Universidad Simon Bolivar, 2016.

[20] S. O. Akande, "Dimensional Accuracy and Surface Finish Optimization of Fused Deposition Modelling Parts using Desirability Function Analysis," International Journal of Engineering Research & Technology, Vol. 4, April 2015.

[21] D. E. Hardt, *Cycle To Cycle Control: Cycle To Cycle Control: The Case for using Feedback and SPC The Case for using Feedback and SPC*, MIT, [Online], <https://ocw.mit.edu/courses/mechanical-engineering/2-830j-control-of-manufacturing-processes-sma-6303-spring-2008/lecture-videos/lecture20.pdf,Accessed20July2017,May2008>.

[22] D. E. Hardt and T.-S. Siu, "Cycle to cycle manufacturing process control," found in *Innovation in Manufacturing Systems and Technology (IMST)*, Jan. 2002.

[23] Winter, *Lecture 5 - Feedforward*, Stanford, <https://web.stanford.edu/class/archive/ee/ee392m/ee392m.1034/Lecture5_Feedfrwrd.pdf>, Available: 3 August 2017.

[24] D. Montgomery, *Introduction to Statistical Quality Control*, Wiley, 2009, 6th ed., pp 549-594.

[25] "User Manual for 3D Coordinate Metrology," TESA Technology, Internal document used by NVBOTS.

[26] *Micro-Hite 3D CMM*,[Online], <http://www.microhite3dcmm.com/>. Accessed: 30 May 2017.

[27] *3.3 - Prediction Interval for a New Response*, PennState Elberly College of Science, STAT 501, 2017, <https://onlinecourses.science.psu.edu/stat501/node/274>, Accessed: 11 July 2017.

[28] *Confidence and Prediction Bounds - MATLAB & Simulink*, <https://www.mathworks.com/help/curvefit/confidence-and-prediction-bounds.html>, Accessed: 27 July 2017.

[29] *Analysis of Covariance - MATLAB & Simulink*, <https://www.mathworks.com/help/stats/analysis-of-covariance.html>, Accessed: 2 August 2017.

Appendices

Drawing specific to fast quality PLA parts.

For ABS+ parts, heights need to be adjusted to account for different nominal layer thickness

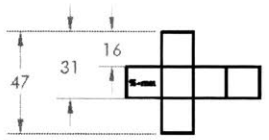

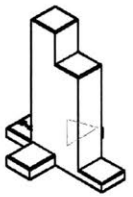

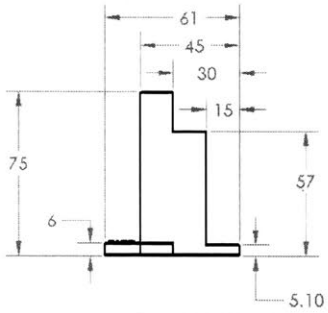

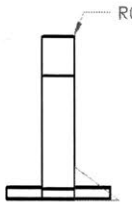

UNLESS OTHERWISE SPECIFIED:		NAME	DATE
DIMENSIONS ARE IN INCHES	DRAWN		
TOLERANCES: FRACTIONAL ± ANGULAR: MACH ± BEND ± TWO PLACE DECIMAL ± THREE PLACE DECIMAL ±	CHECKED		
	ENG APPR.		
	MFG APPR.		
INTERPRET GEOMETRIC TOLERANCING PER:	Q.A.		
MATERIAL	COMMENTS:		
FINISH			
NEXT ASSY / USED ON			
APPLICATION / DO NOT SCALE DRAWING			

TITLE:

SIZE DWG. NO. REV
A Proposed_column_design
SCALE: 1:2 WEIGHT: SHEET 1 OF 1

Proposed Fixture Part